

Mean Inner Potential MIP = $\Phi_0 = V_0$

- Why?

Refraction
Thickness & Shape
Composition
Work function & Fermi energy
Bond energy

- How?

Interferometry / Holography

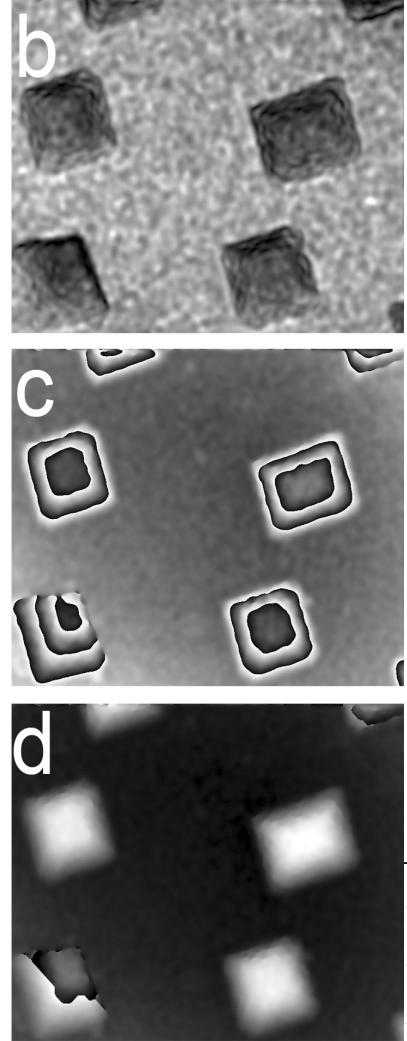
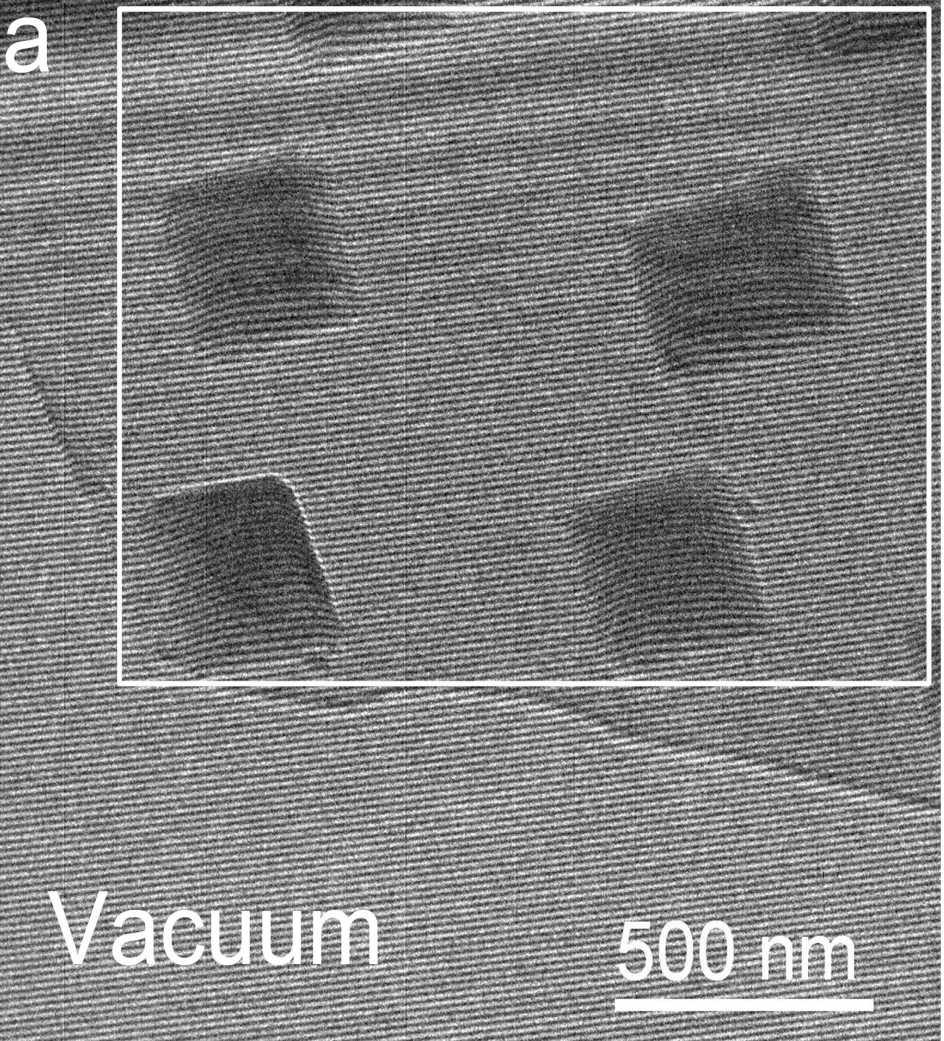
$$\varphi = \sigma V_0 t$$

- Faq?

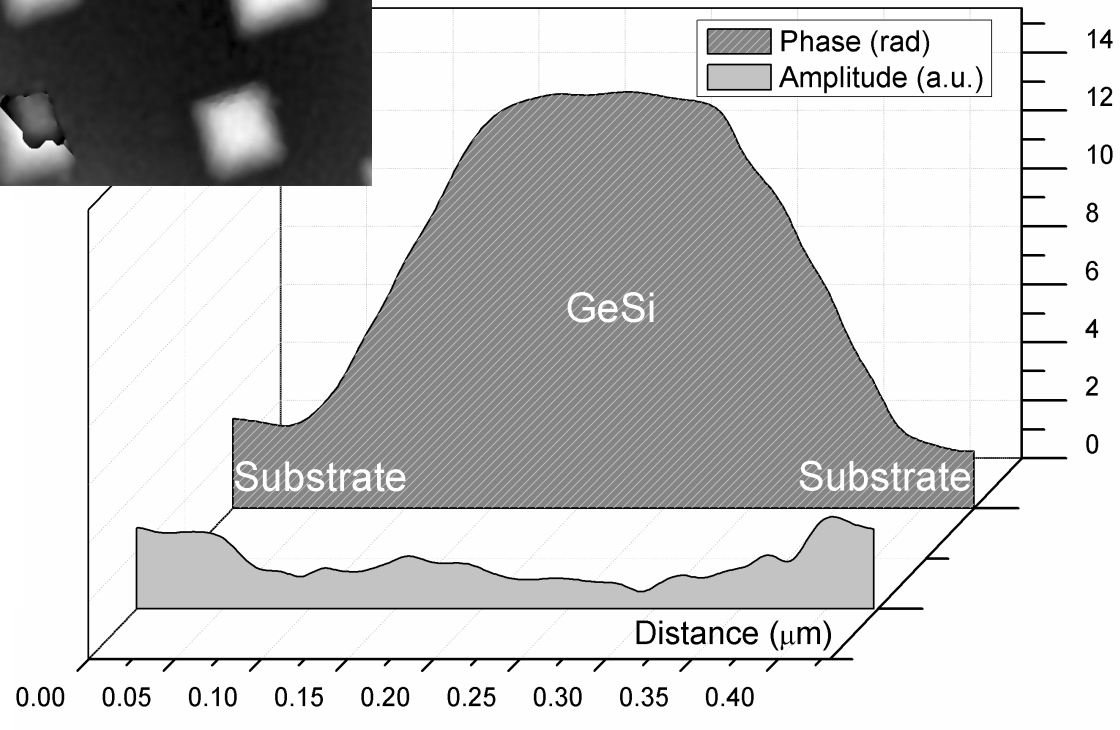
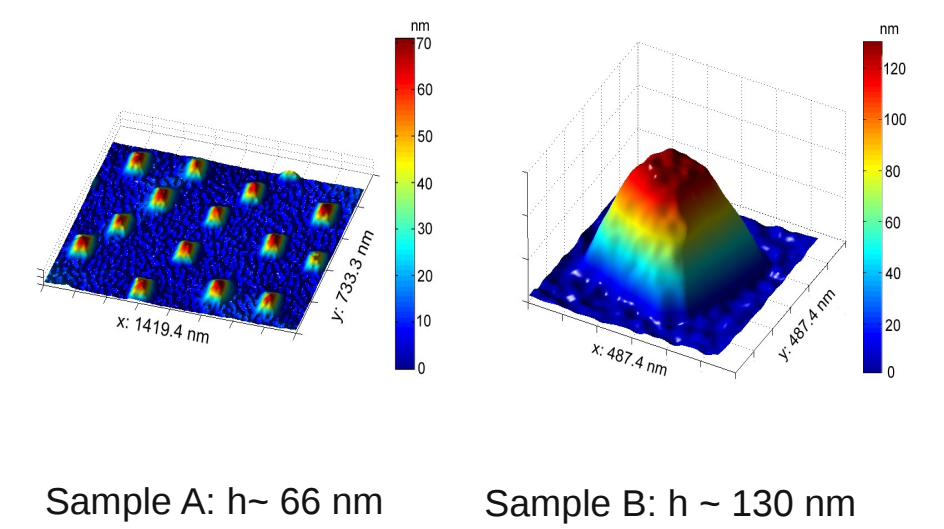
Inverse problem: Uniqueness
Strain / Stress / Defects

$$\Psi \sim e^{i\pi A t} \sim e^{iV_0 t} \cdot e^{-\mu t} \cdot (1 + i\pi A' t + \dots)$$

Reconstruction of (Si,Ge) islands



- a hologram
- b amplitude
- c phase
- d unwrapped phase



Die dynamische Theorie der Elektronen-Interferenzen.

§ 18. Das mittlere Potential im Raumgitter¹⁾.

Wir können nämlich zeigen, daß es für ein
bis an seine Ränder ungestörtes Raumgitter im allgemeinen kein solches
Potential gibt.

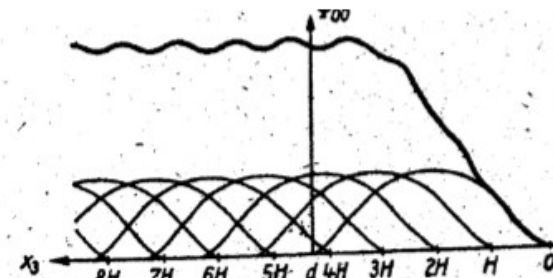


Fig. 108. Entstehung des Flächenmittels $\varphi_{00}(\bar{x})$ durch Überlagerung von vier Kurven $\varphi_{00}(x)$.

Gleichgültig, wie viele Kurven $\varphi_{00}(x)$ sich überlagern, zwischen welchen Werten also die ganze Zahl m laufen muß, immer gilt danach

$$\varphi_{00\bar{0}} = \frac{1}{H} \int_0^d \varphi_{00}(x_3) dx_3; \quad (18.14)$$

- SCF with ρ of isolated atoms insufficient
- DFT very extensive for larger structures
- MD with analytical bond order potential

$$E_{\text{tot}} = E_{\text{rep}} + E_{\text{prom}} + \sum H_{i\alpha,j\alpha} \Theta_{i\alpha,j\alpha}$$

empirical
 $s^2p^2 \rightarrow sp^3$
band energy replaced by hopping
integrals and bond order matrix

On the Average Coulomb Potential (Φ_0) and Constraints on the Electron Density in Crystals

In this paper, we argue that the average potential in a finite crystal is a well defined quantity, but that extending the concept to an infinite crystal can lead to incorrect conclusions. ^{cell}

However, the evaluation of V_0 using this expression ignores any surface effects, the ambiguity about the point of zero potential in an infinite crystal and leaves open the question of whether $V(r)$ can be obtained from the knowledge of $\rho(r)$ alone for an infinite crystal.

For the case of a finite crystal with boundary condition of zero potential at infinity, the potential is completely defined by the charge distribution $\rho(r)$ using Poisson equation. The correct procedure for defining V_0 is then to average the potential of the finite crystal according to [11,12], which is given by

$$V_0 \equiv -\frac{1}{\Omega_{\text{cryst}}} \iint \frac{\rho(r)}{|r - r'|} dr' dr = \frac{2\pi}{3\Omega_{\text{cryst}}} \int r'^2 \rho(r') dr'. \quad (4)$$

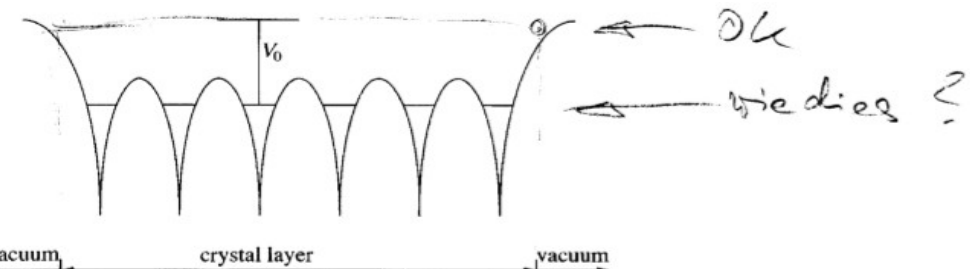


Fig. 1. Coulomb potential $V(z)$ for silicon (d) in Table 1 plotted as a function of distance through the slab. The method of defining V_0 is indicated. For silicon (110), the crystal layer width of a unit cell is 0.21 nm^2 . The laterally-averaged potential falls to less than 0.02 V within a distance of 0.37 nm from the nuclei of the surface atoms, measured normal to the surface

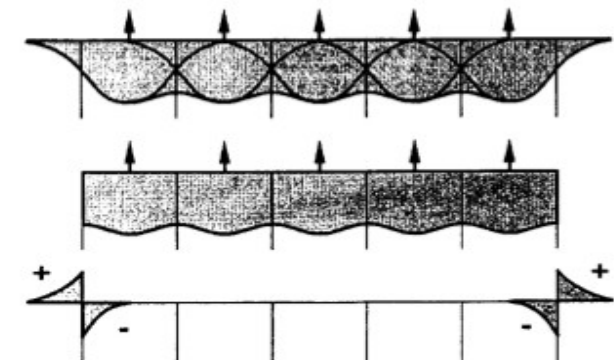
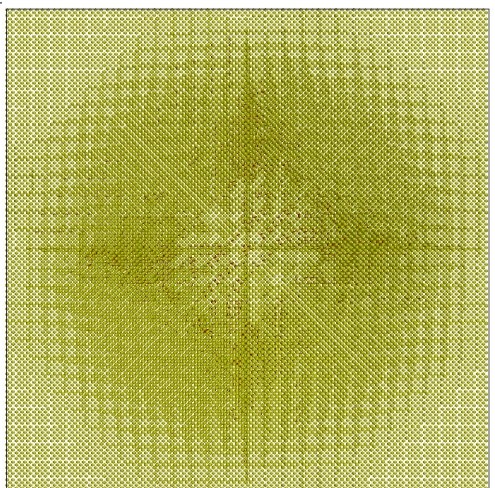
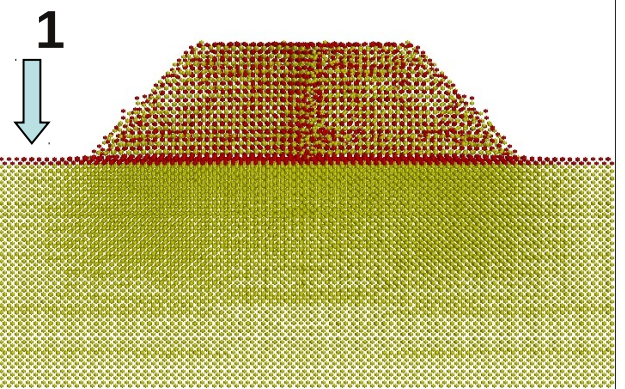
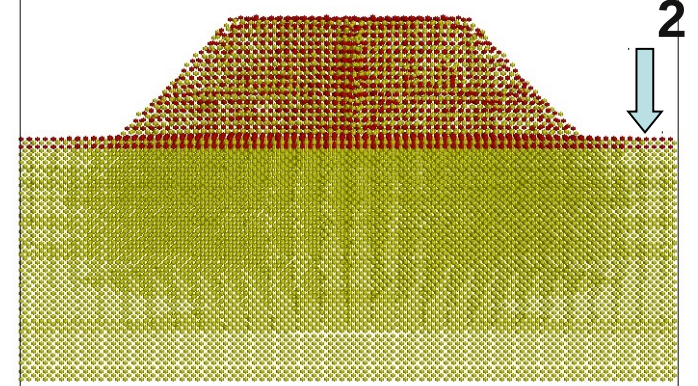
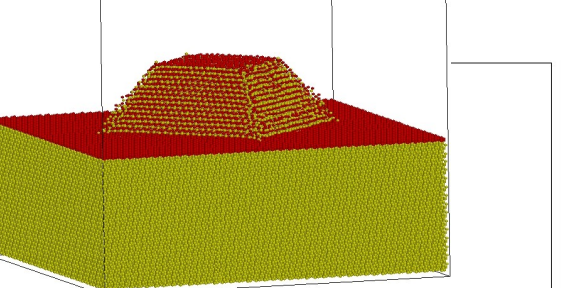
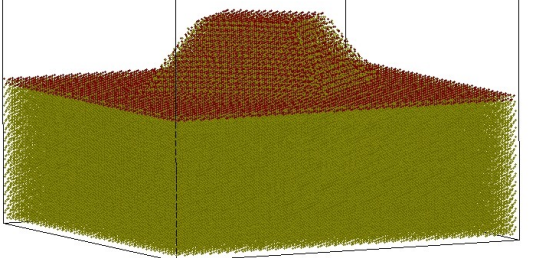
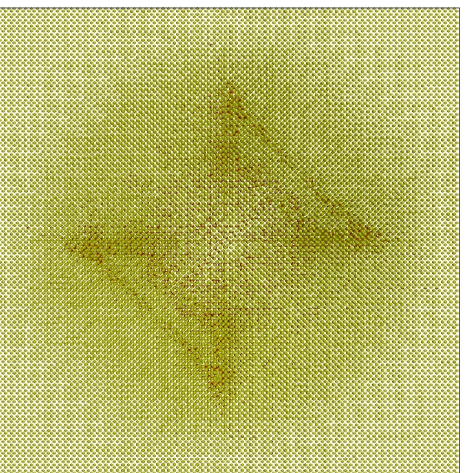


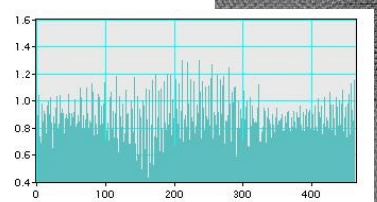
Fig. 7. Comparison of two ways of assembling a crystallite from bases. Top: charge density in a crystallite of pseudo-atoms. Middle: the charge density as an assembly of unit cells. Bottom: the difference showing the surface dipole layer. The arrows indicate the positions of the nuclei of the pseudo-atoms.



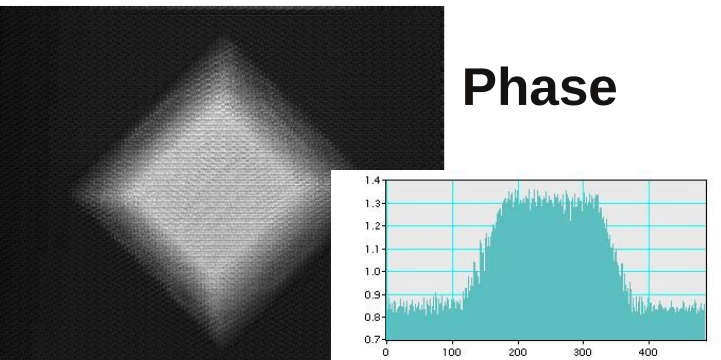
**SiGeQD
MDrelaxed
&
simulated
exit wave**



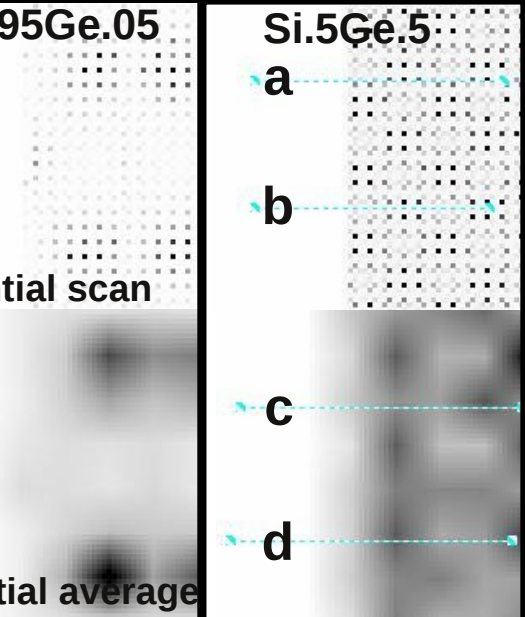
Amp



Phase

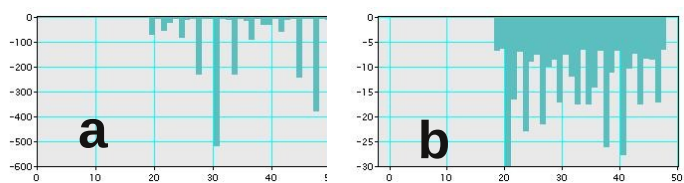


Si.95Ge.05



potential scan

potential average

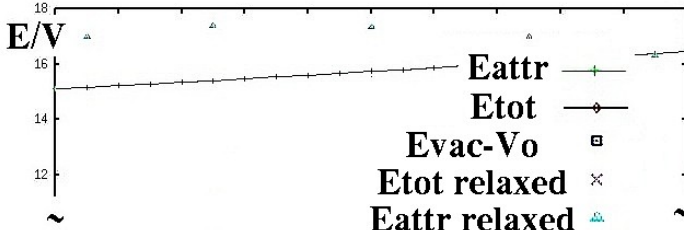


a

b

c

d



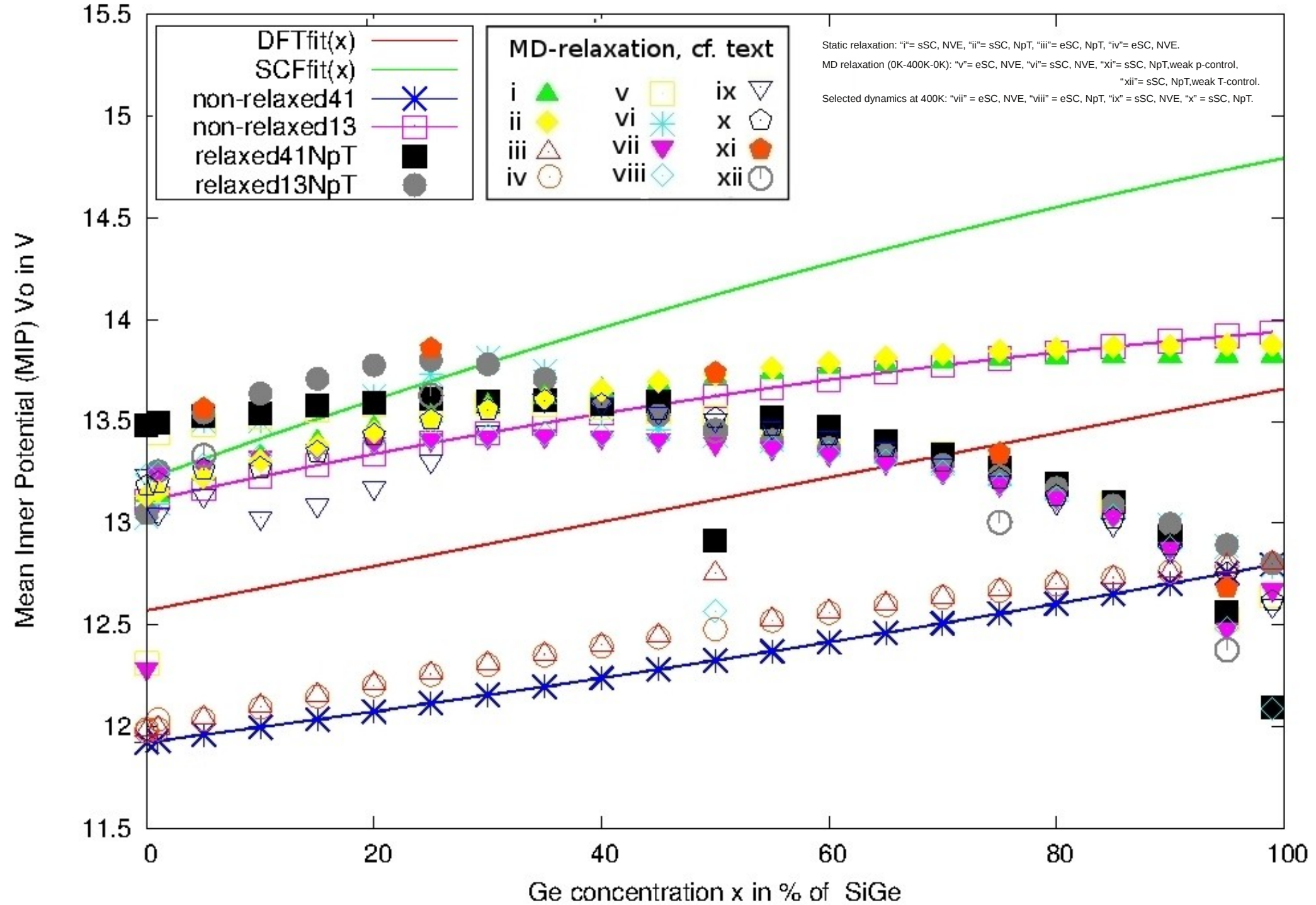
Eattr

Etot

Evac-Vo

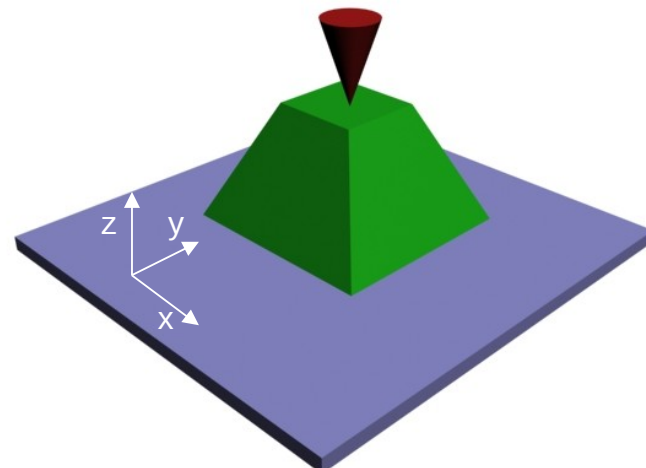
Etot relaxed

Eattr relaxed



Goal: Analyzing 3D (Si,Ge) nanostructures

STM and AFM



Composition, structure, strain, morphology
of (Si,Ge) nanostructures

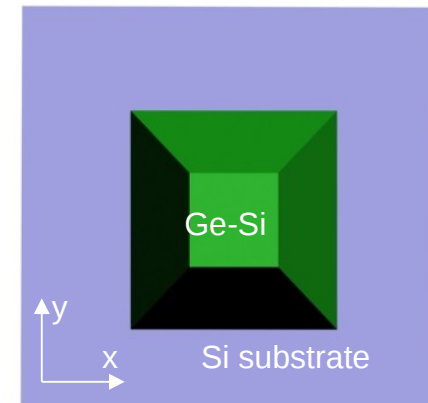


Physical properties
(confinement)



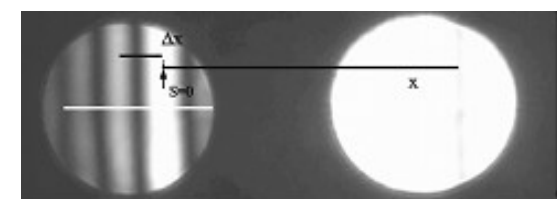
Applicability electronic / photonic
devices

(C)TEM

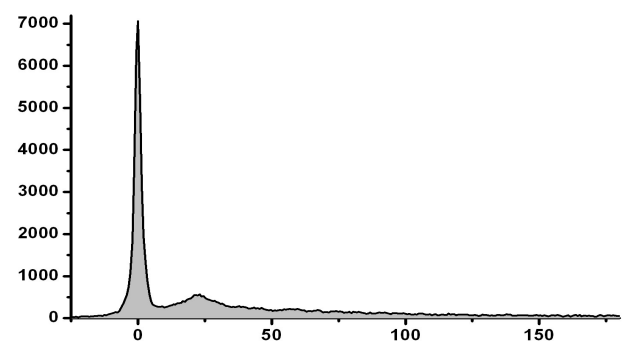


CTEM: two dimensional projection
dynamical diffraction complexity

CBED

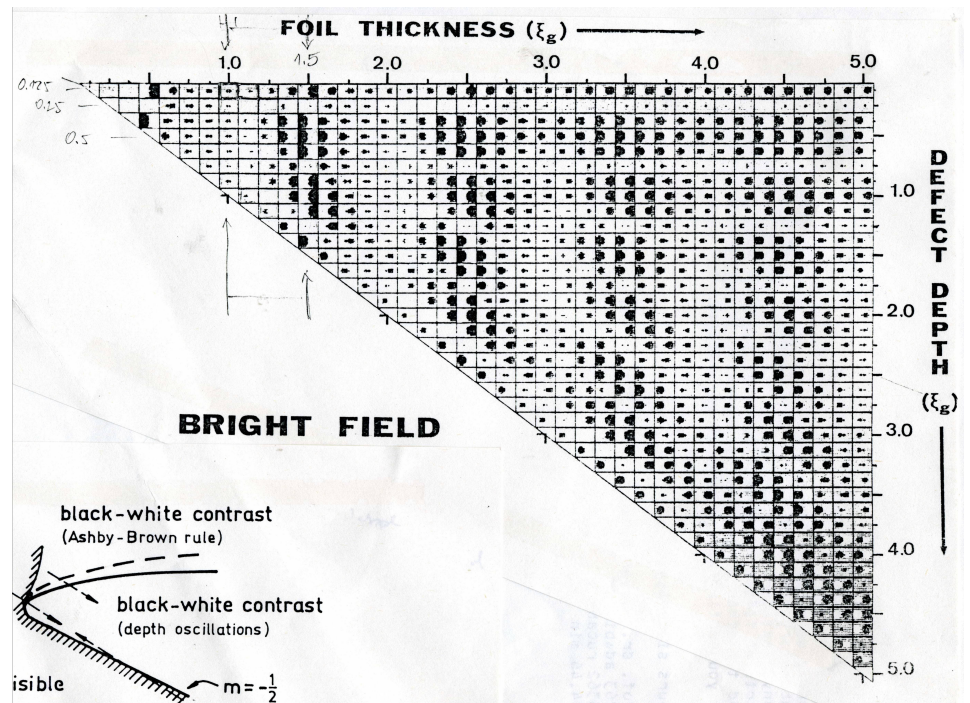
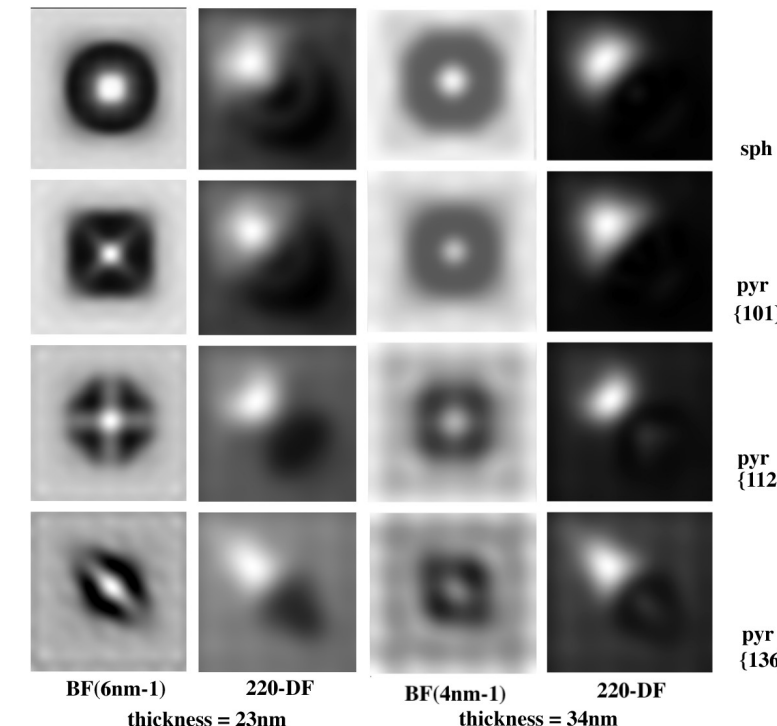
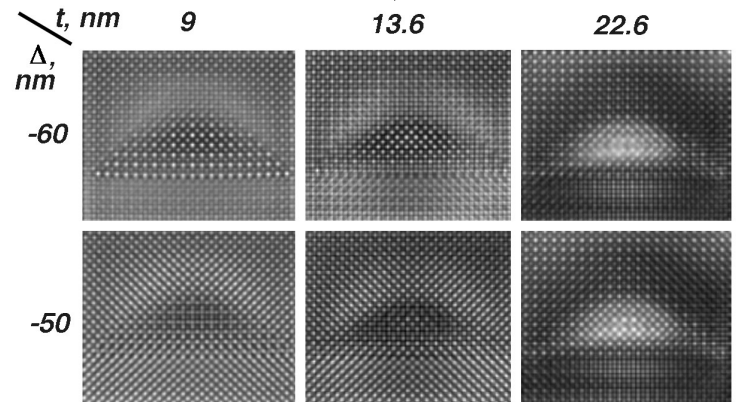
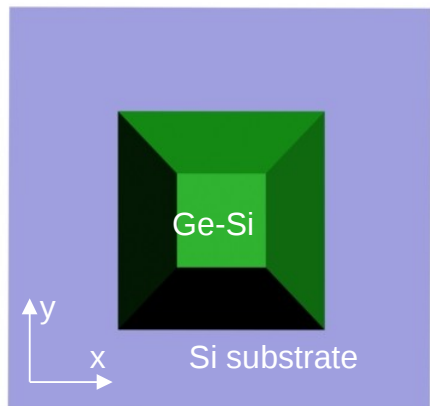
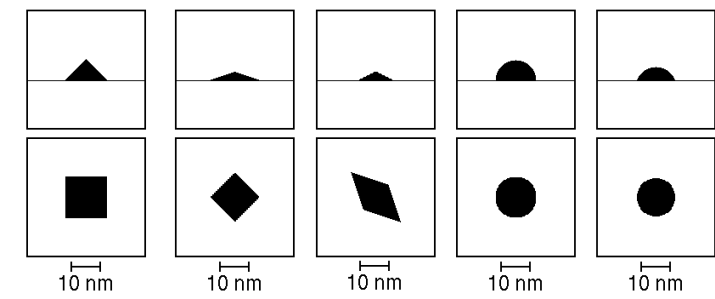


EELS

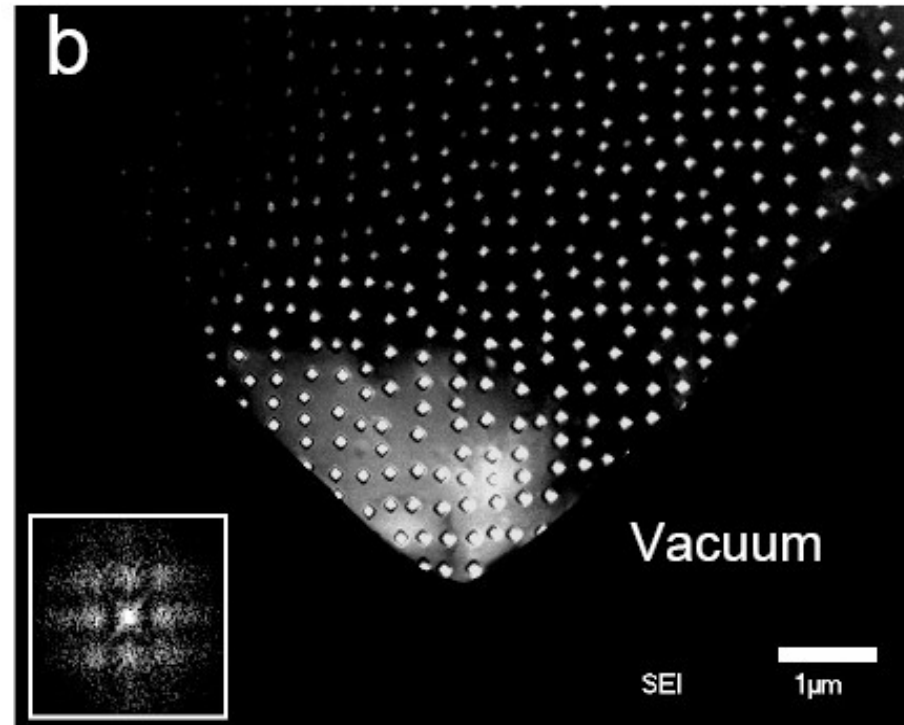


Analyzing TEM of 3D (Si,Ge) nanostructures

(C)TEM



STEM-HAADF and BF-TEM of (Si,Ge) islands:

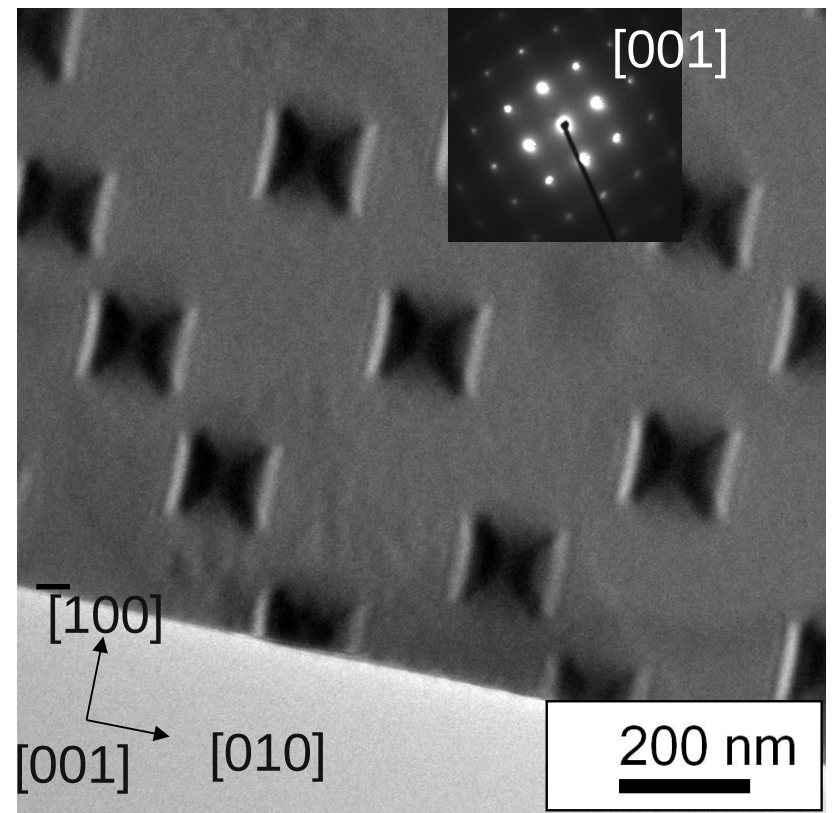
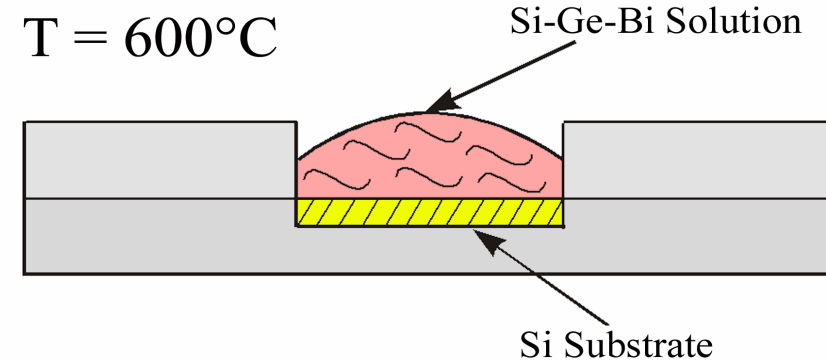


STEM-HAADF image

Sample A

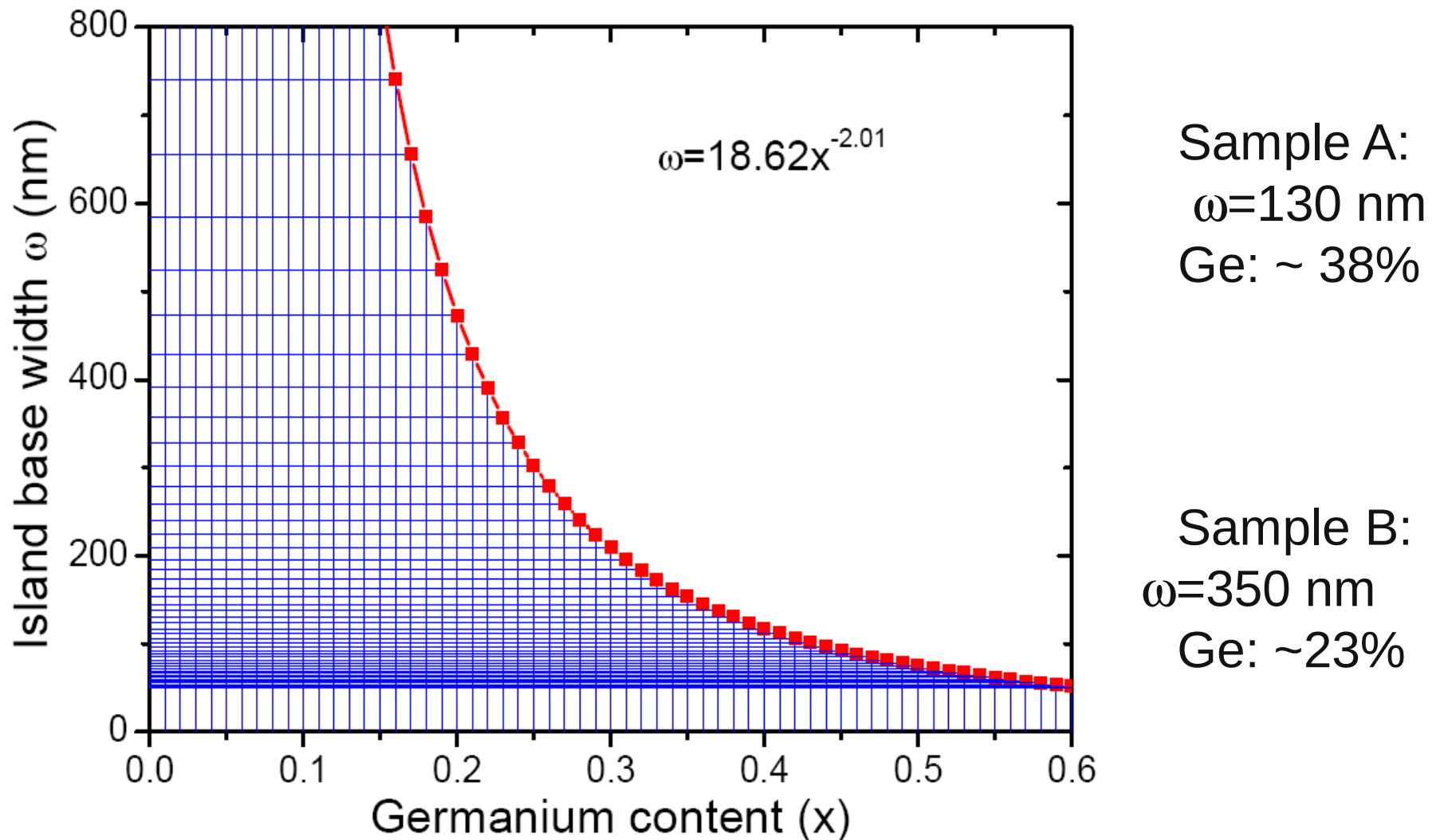
CTEM image

Liquid phase epitaxy growth

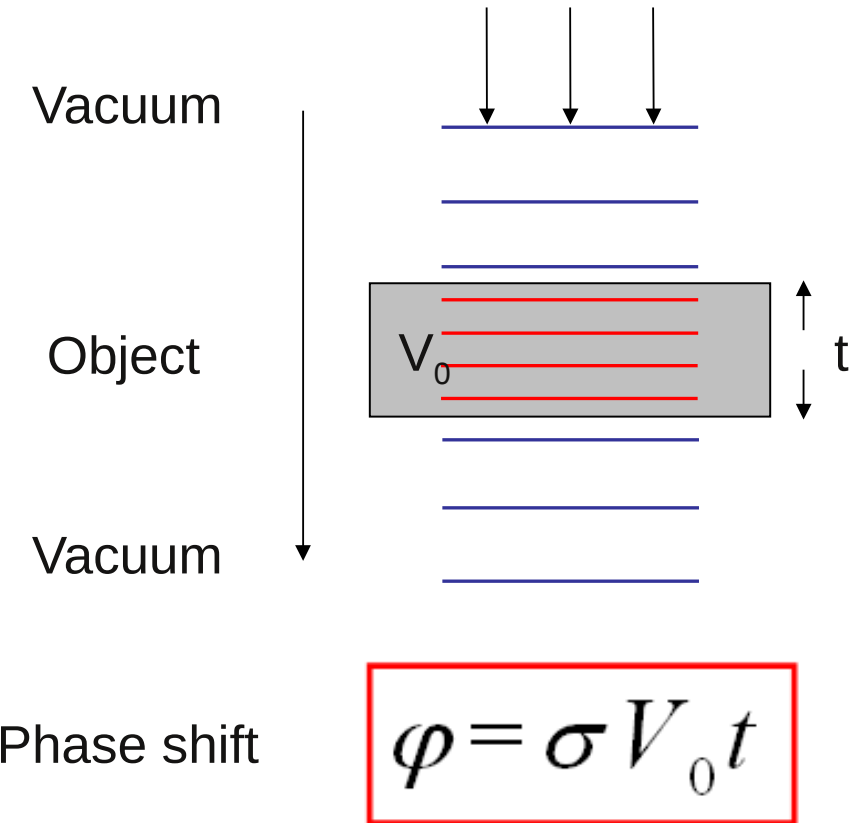


LPE grown $\text{Si}_{1-x}\text{Ge}_x$ islands

Ge concentration x vs. base plane width ω

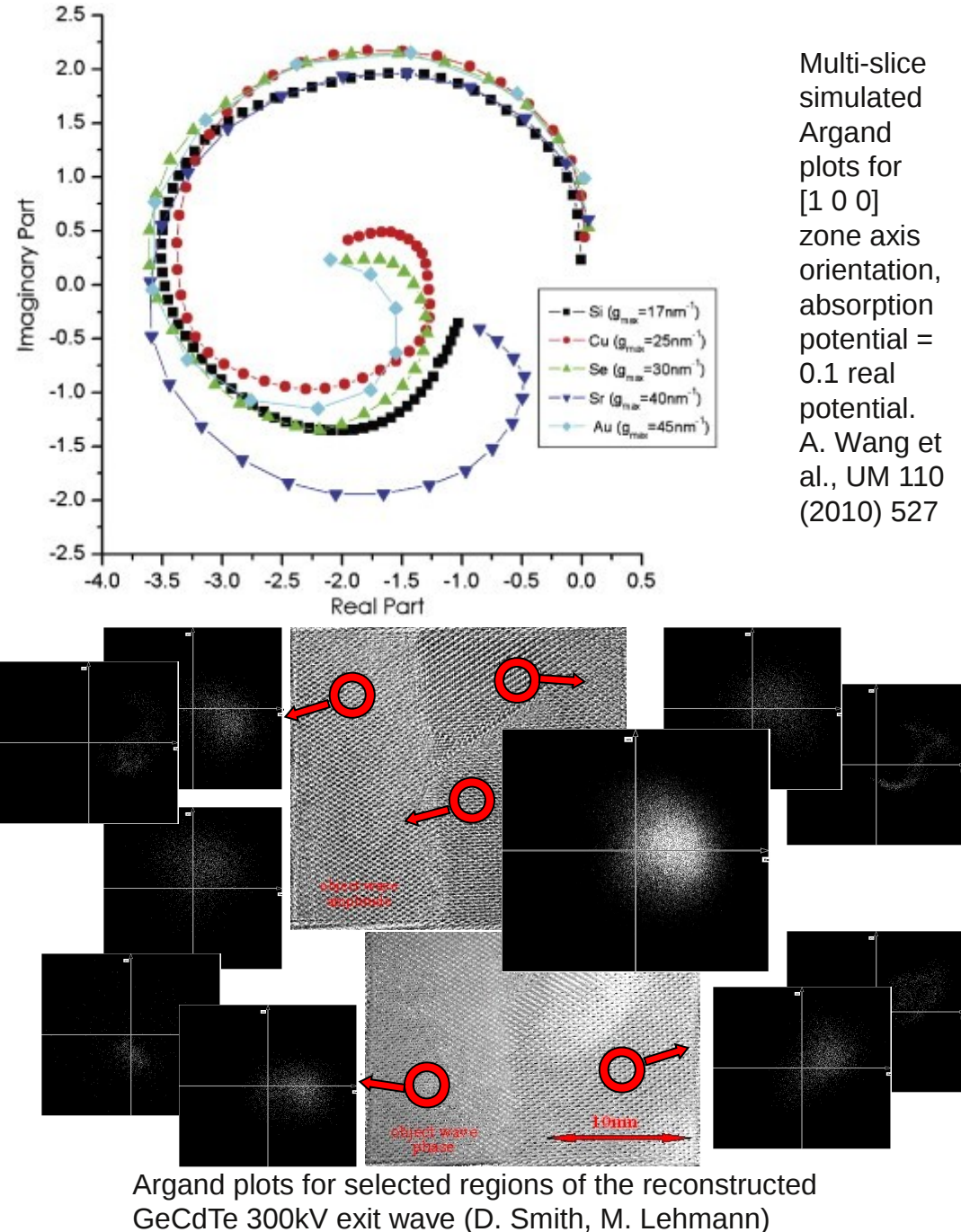


High energy electrons: Phase grating approximation

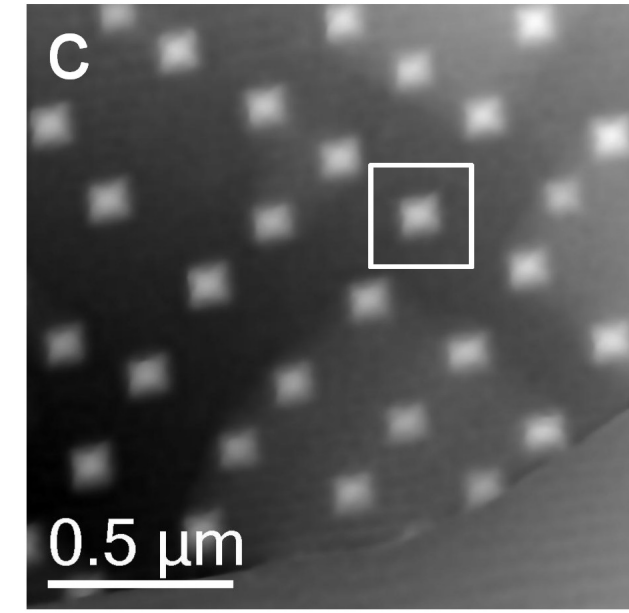
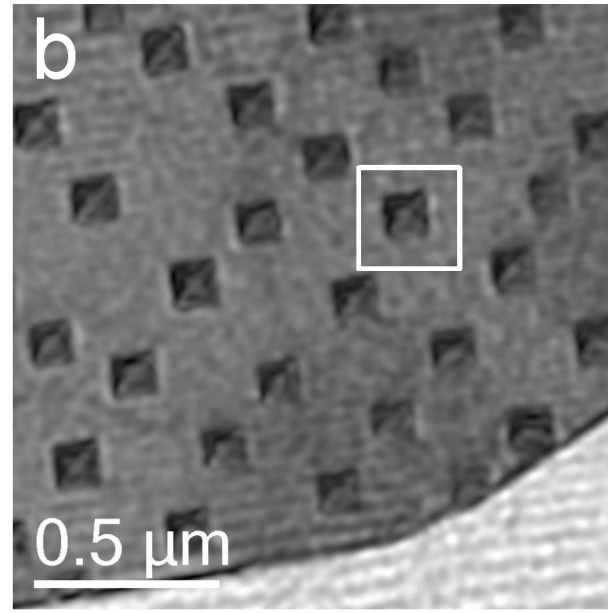
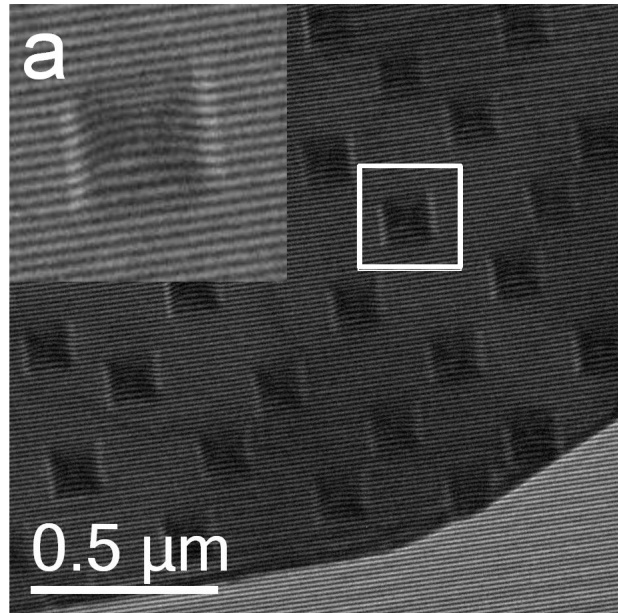


V_0 : Mean inner Coulomb potential
 t : Object thickness

$$\sigma = \frac{2\pi}{\lambda V} \left(\frac{m_0 c^2 + eV}{2m_0 c^2 + eV} \right) = \frac{2\pi m e \lambda}{h^2}$$



Electron holography of (Si,Ge) islands

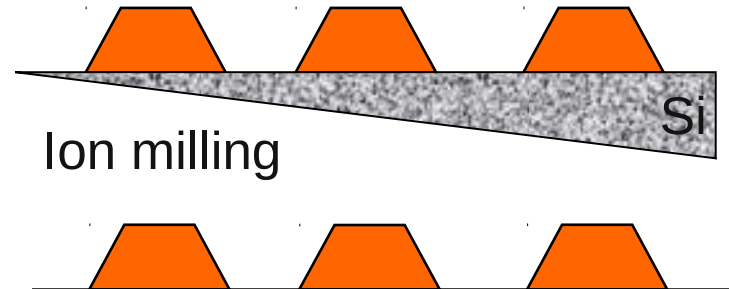


Electron hologram

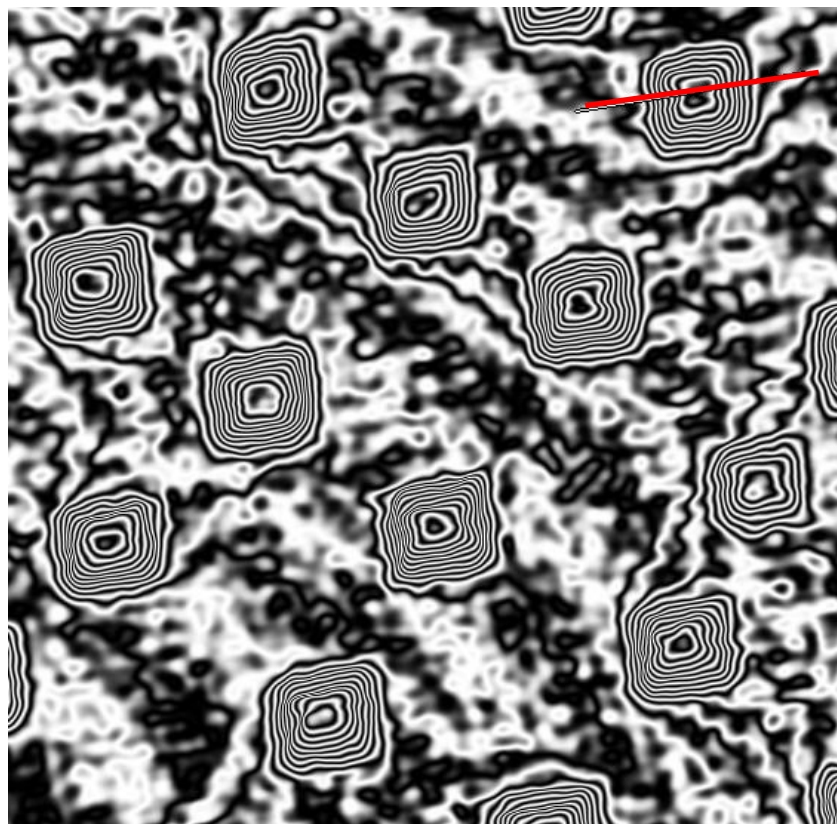
Amplitude

Unwrapped phase

Sample A

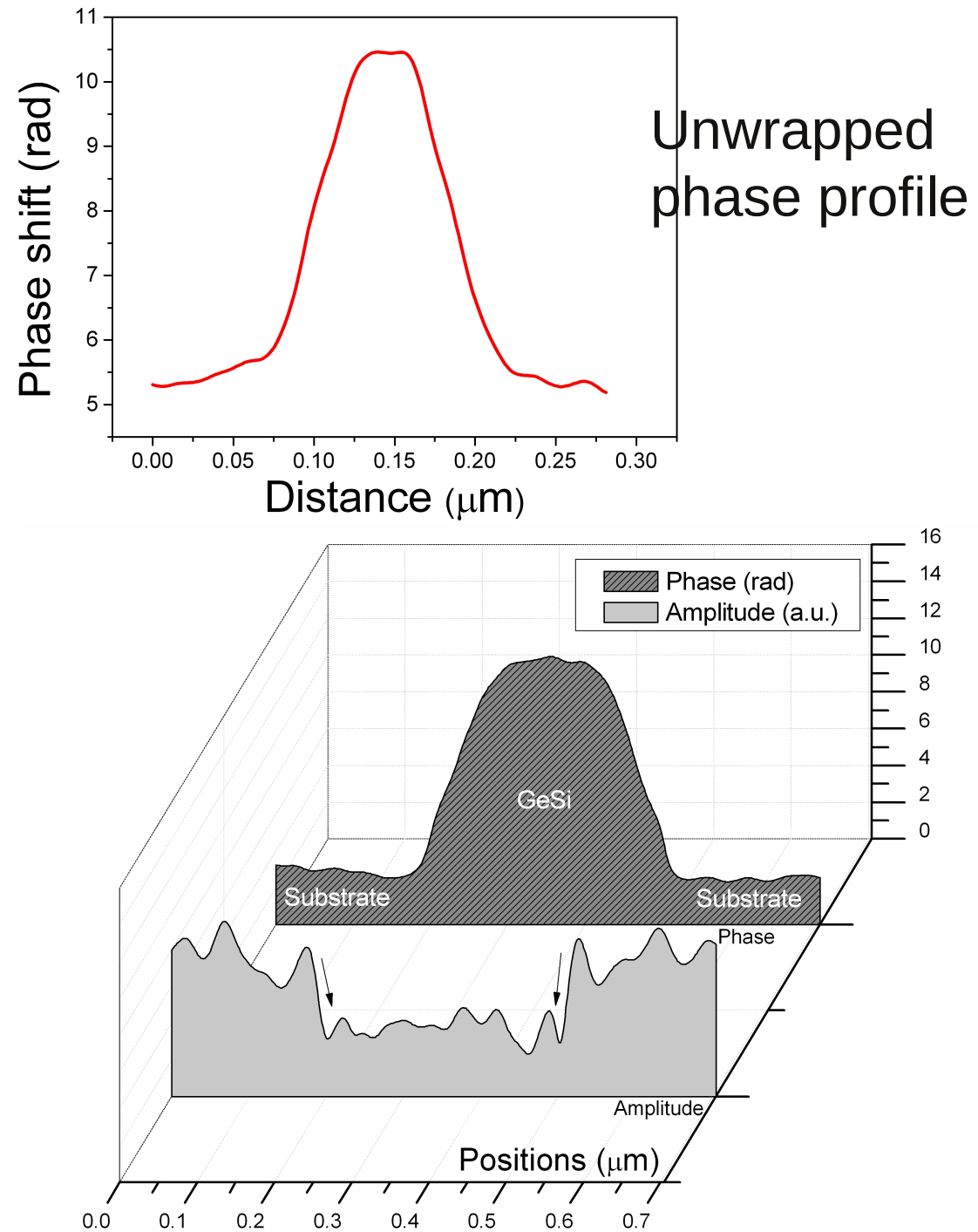


Amplified phase image of (Si,Ge) islands



10 × amplified phase image

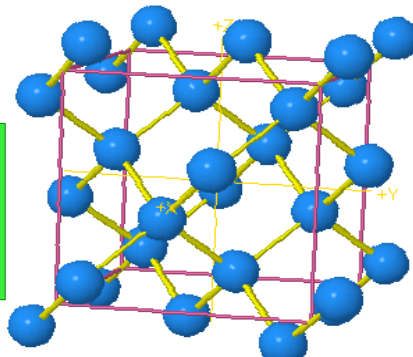
Sample A



Mean inner potential (MIP) & atomic scattering factors

MIP

$$V_0 = -\frac{1}{\Omega} \int V(r) d^3r$$



atomic scattering & structure factor

$$f(0) = -\frac{m\Omega}{2\pi\hbar^2} V_0$$

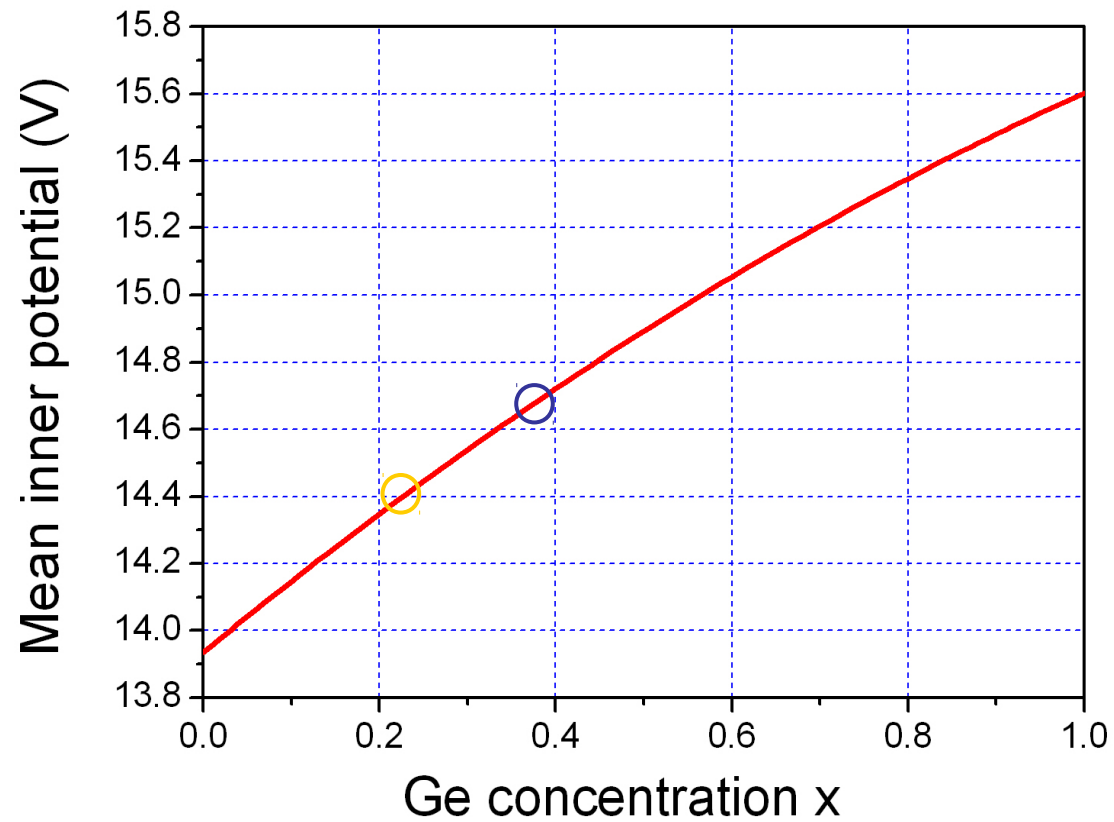


$$f_{\text{Si}}(0) = 5.828 \text{\AA} \quad f_{\text{Ge}}(0) = 7.378 \text{\AA}$$

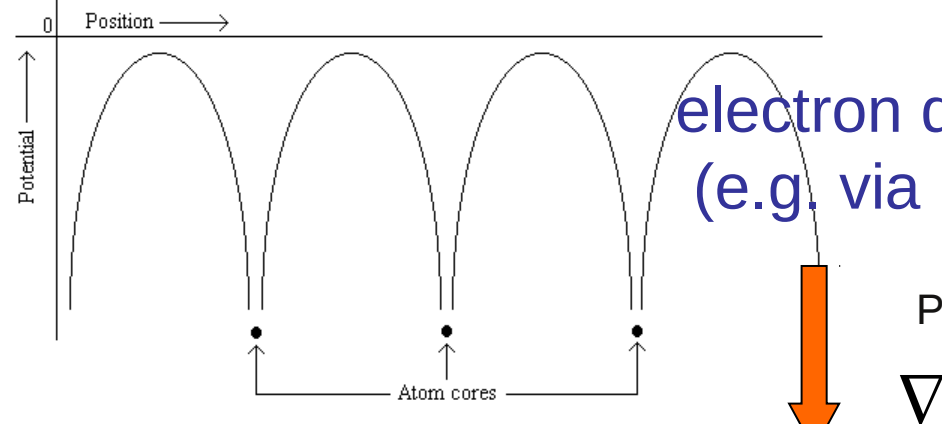
$$V_0 = \frac{h^2}{2\pi me\Omega} \sum_i n_j f_{el}^j$$

Lattice parameter:
 $a = (5.431 + 0.20x + 0.027x^2) \text{\AA}$

J.P.Dismukes, et al.. *J. Appl. Phys.* **35**(1964)2899.



bonding & electron interaction effects

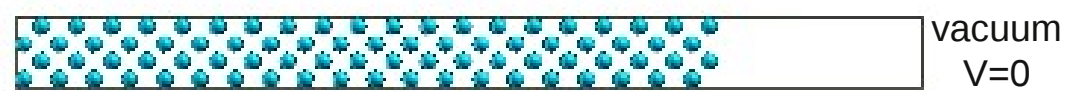
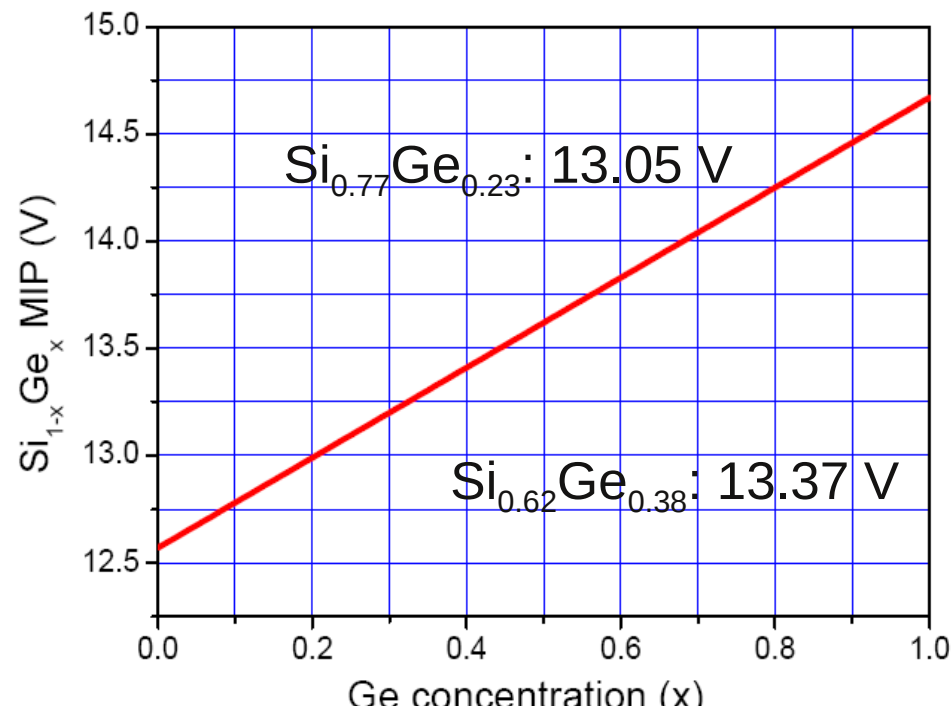
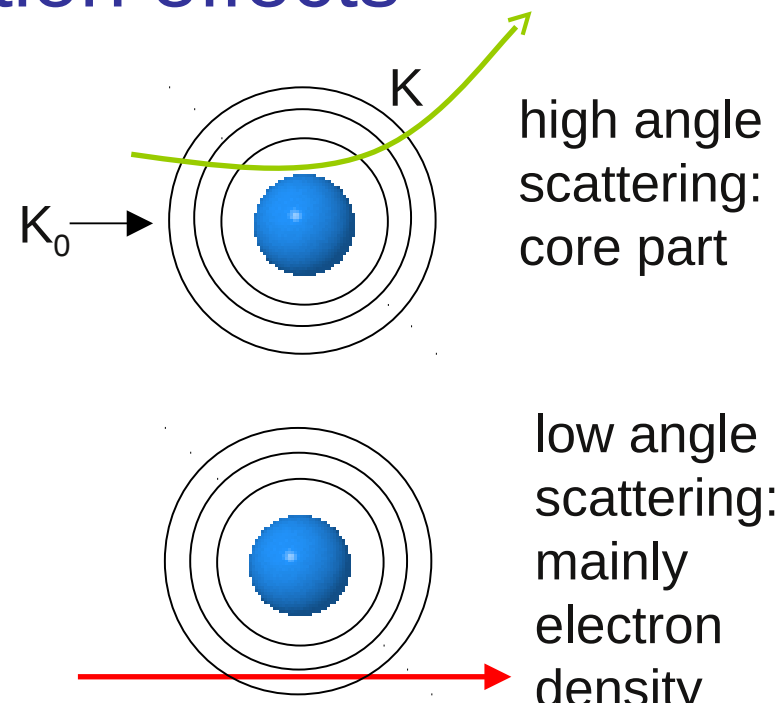


electron density (e.g. via DFT)

Poisson equation

$$\nabla^2 \varphi = -\frac{\rho}{\epsilon_0}$$

electric potential



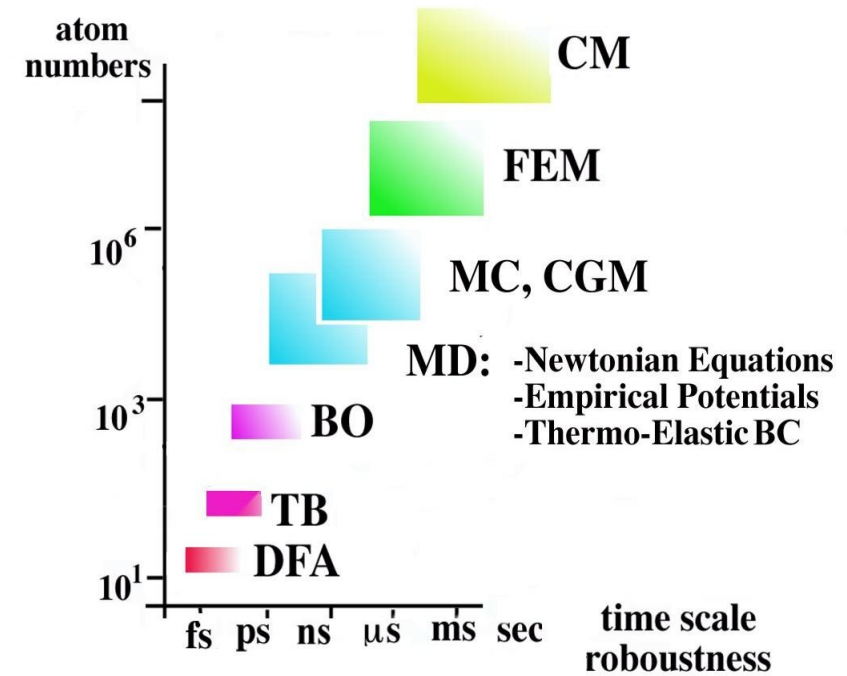
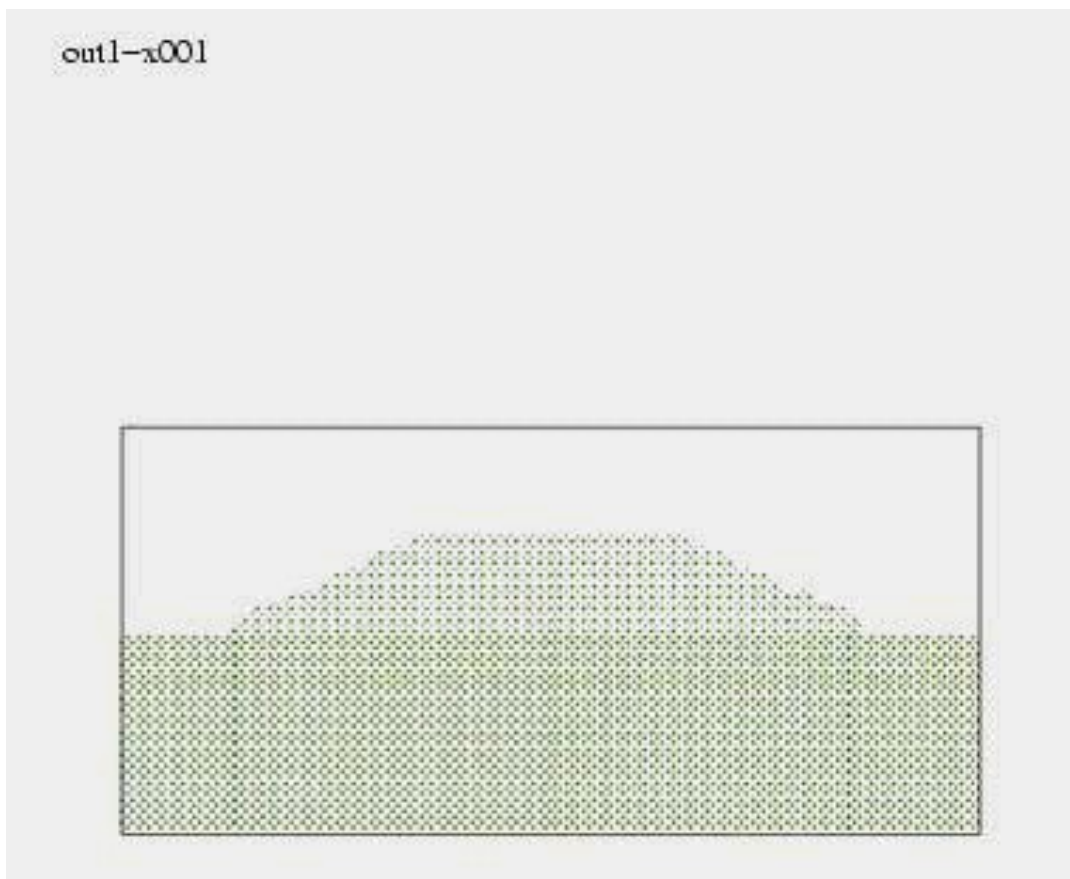
electron density from unit to super cell

	DFT(V)	No-bonding (V)
Si	12.57	13.91
Ge	14.67	15.58

Classical molecular dynamics

time-integration (fs-steps) up to relaxation (< 1ns)
simultaneously 3N Newtonian equations of motion
with **V= empirical interaction potential**

$$m_j \frac{d^2 r_j}{dt^2} = F_j = -\frac{\partial V}{\partial r_j}$$



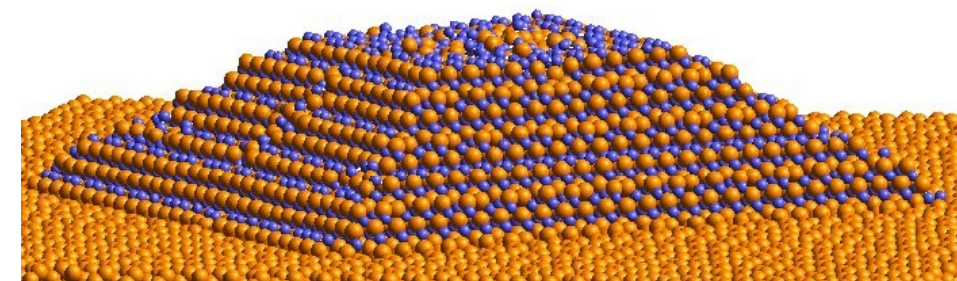
Relaxation of an uncapped
(100)-SiGe/Si pyramid
 $\Delta\Delta T = 20K/ns$ up/down

$$\Delta t = 0.1\text{fs}$$

$$T_{\max} = 900\text{K}$$

$$\Delta t_{\text{equil}} = 1\text{ns}$$

$$\Delta t_{\text{frame}} = 0.1\text{ns}$$



BOP

embedded bonds instead atoms – two-center orthogonal TB
density matrix instead diagonalisation – Lanczos recursion

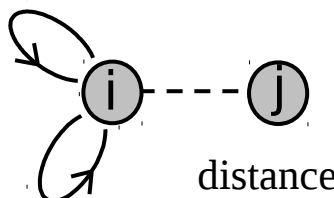
$$E_{\text{tot}} = E_{\text{rep}} + E_{\text{prom}} + E_{\text{band}}(k)$$

\downarrow \downarrow \downarrow

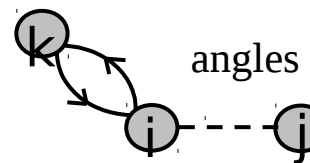
$$\text{empirical} \quad s^2p^2 \rightarrow sp^3 \quad \sum H_{i\alpha,j\alpha} \Theta_{i\alpha,j\alpha}$$

\downarrow \downarrow

hopping integrals BOmatrix Pettifor-Aoki
Slater-Koster ssσ, spσ, ppσ...
electronic hopping in closed loops



$$\Phi_{2\sigma}^i = \hat{\delta}_i^2 + \sum_{k(i)} \hat{\beta}_{\sigma,ik}^2 (g_{\sigma,jik}^2 + g_{\pi,jik}^2)$$

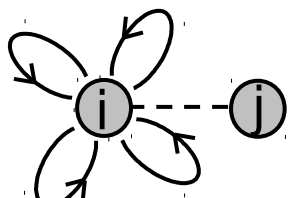


angles

$$\delta_i = E_p - E_s$$

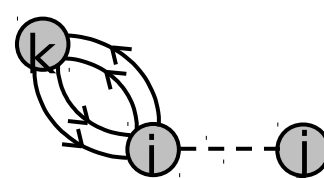
$$g_{\sigma,jik} = 1 + (\cos \theta_{jik} - 1) p_{\sigma,i}$$

$$g_{\varphi,jl} = p_{\pi,ik} \sqrt{p_{\sigma,i} p_{\sigma,k}} \cos \varphi_{jl} \sin \theta_{jik} \sin \theta_{ikl}$$

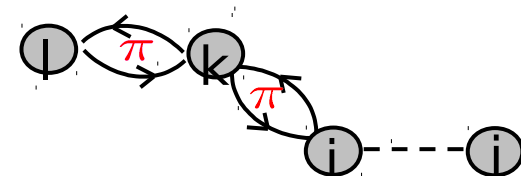


$$\Phi_{4\sigma}^i = \hat{\delta}_i^4 + \hat{\beta}_{\sigma,ik}^4 g_{\sigma,jik}^2 + \dots +$$

dihedral „, torsion



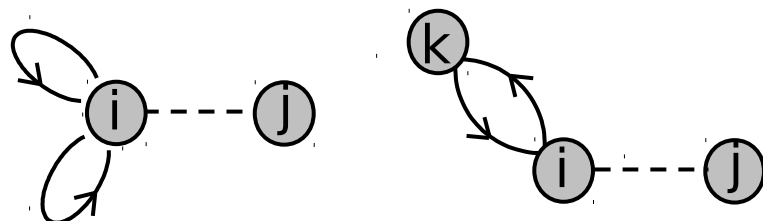
$$\hat{\beta}_{\sigma,ik}^2 \hat{\beta}_{\sigma,kl}^2 [2g_{\sigma,jik} g_{\sigma,ikl} + g_{\varphi,jl}] g_{\varphi,jl}$$



Bond Order Potential

- Slater-Koster products = electronic hoppings in closed loops

$$\Phi_{n\sigma}^i(a_i, b_i) \Rightarrow \sum_{\alpha_1, \dots, \alpha_{n-1}} \langle i\sigma | \hat{H} | \alpha_1 \rangle \langle \alpha_1 | \hat{H} | \alpha_2 \rangle \dots \langle \alpha_{n-1} | \hat{H} | i\sigma \rangle$$



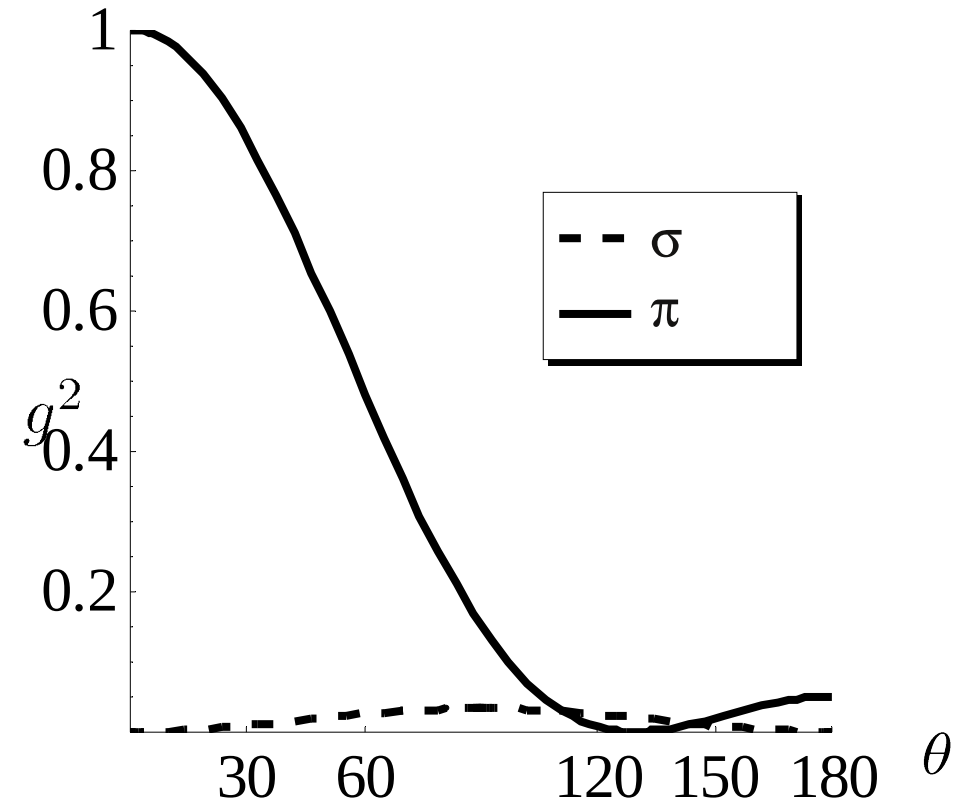
$$\Phi_{2\sigma}^i \propto \langle i\sigma | \hat{H} | i\sigma_0 \rangle^2 + \langle i\sigma | \hat{H} | k \rangle^2$$

On-Site Inter-Site

$$\Phi_{2\sigma}^i = \hat{\delta}_i^2 + \sum_{k(i)} \hat{\beta}_{\sigma,ik}^2 (g_{\sigma,jik}^2 + \cancel{g_{\pi,jik}^2})$$

$$\delta_i = E_p - E_s$$

separation

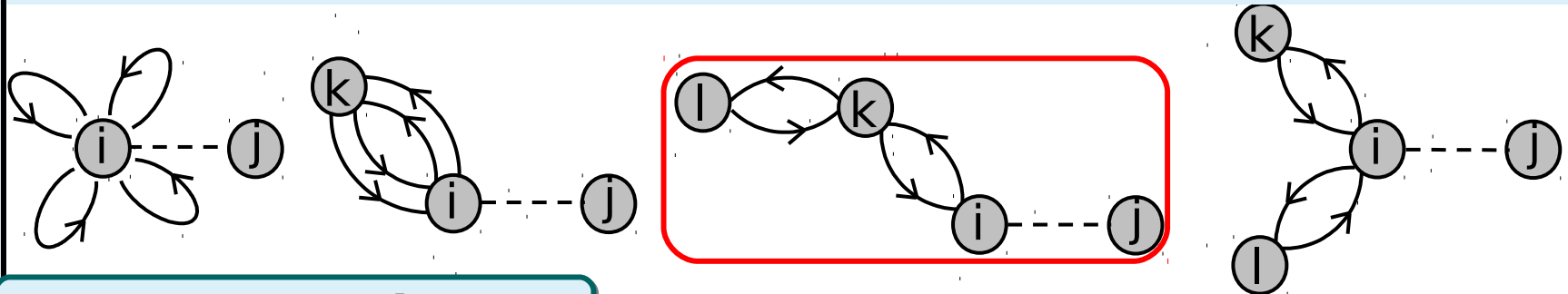


$$g_{\sigma,jik} = 1 + (\cos \theta_{jik} - 1) p_{\sigma,i}$$

angular functions

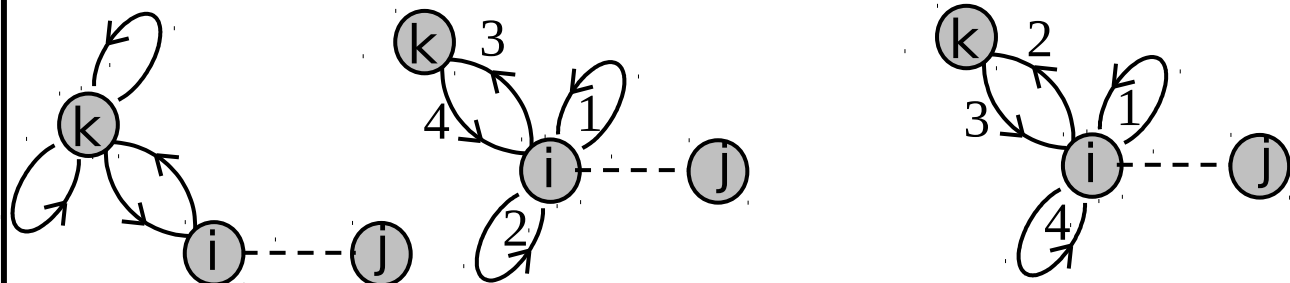
σ & On-Site hops

$$\Phi_{4\sigma}^i = \hat{\delta}_i^4 + \hat{\beta}_{\sigma,ik}^4 g_{\sigma,jik}^2 + \hat{\beta}_{\sigma ik}^2 \hat{\beta}_{\sigma kl}^2 g_{\sigma,jik}^2 g_{\sigma,ikl}^2 + \hat{\beta}_{\sigma,ik}^2 \hat{\beta}_{\sigma,il}^2 g_{\sigma,jik} g_{\sigma,kil} g_{\sigma,jil}$$



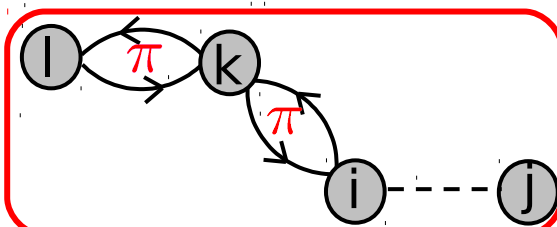
new On-Site hops

$$+ \hat{\beta}_{\sigma,ik}^2 g_{\sigma,jik}^2 (\hat{\delta}_k^2 + 2\hat{\delta}_i^2) + \hat{\beta}_{\sigma,ik}^2 p_{\sigma,i} (1 - p_{\sigma,i}) (1 - \cos \theta_{jik})^2 \hat{\delta}_i^2$$



new π hops

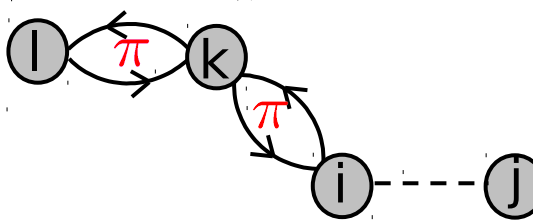
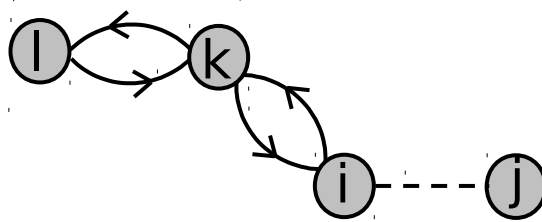
$$+ \hat{\beta}_{\sigma,ik}^2 \hat{\beta}_{\sigma,kl}^2 [2g_{\sigma,jik} g_{\sigma,ikl} + g_{\varphi,jl}] g_{\varphi,jl}$$



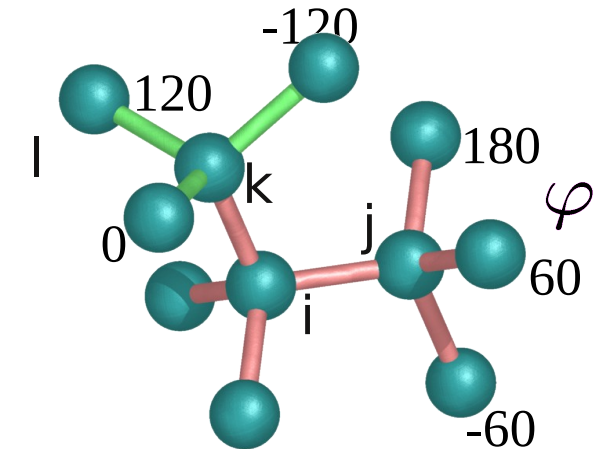
torsion included:

$$g_{\varphi,jl} = p_{\pi,ik} \sqrt{p_{\sigma,i} p_{\sigma,k}} \cos \varphi_{jl} \sin \theta_{jik} \sin \theta_{ikl}$$

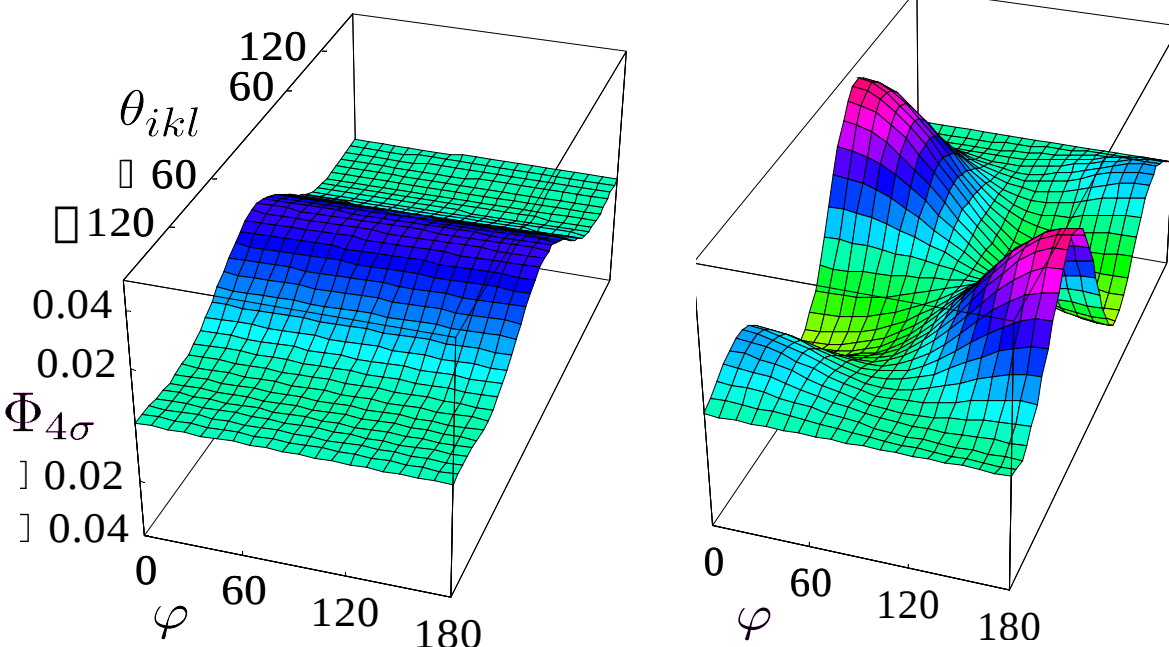
Comparison of π -and σ -contributions



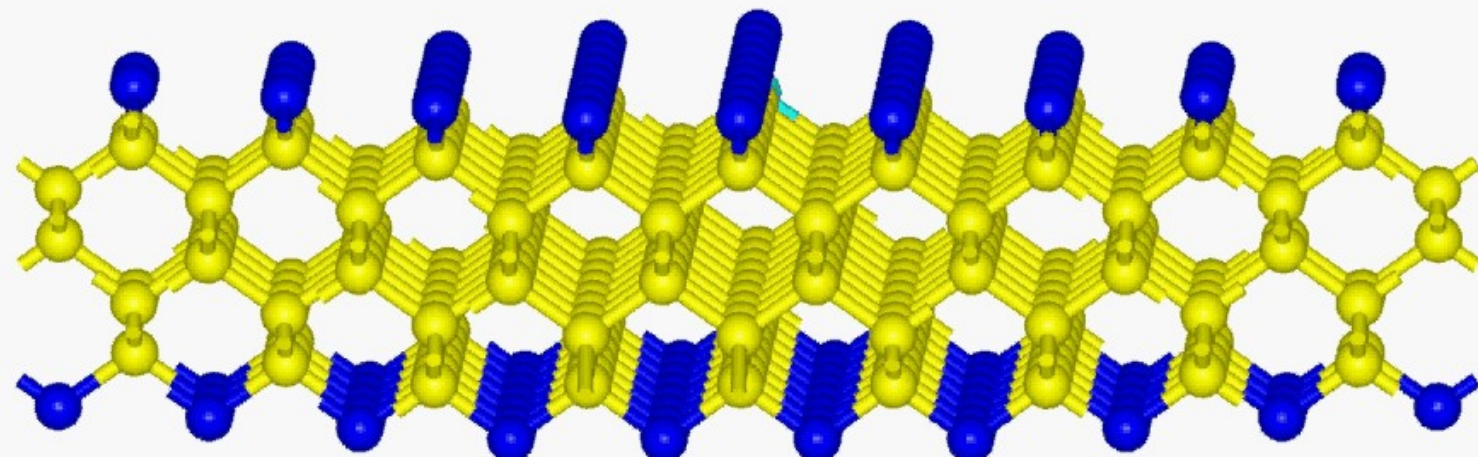
$$\cos \theta_{jik} = -1/3$$



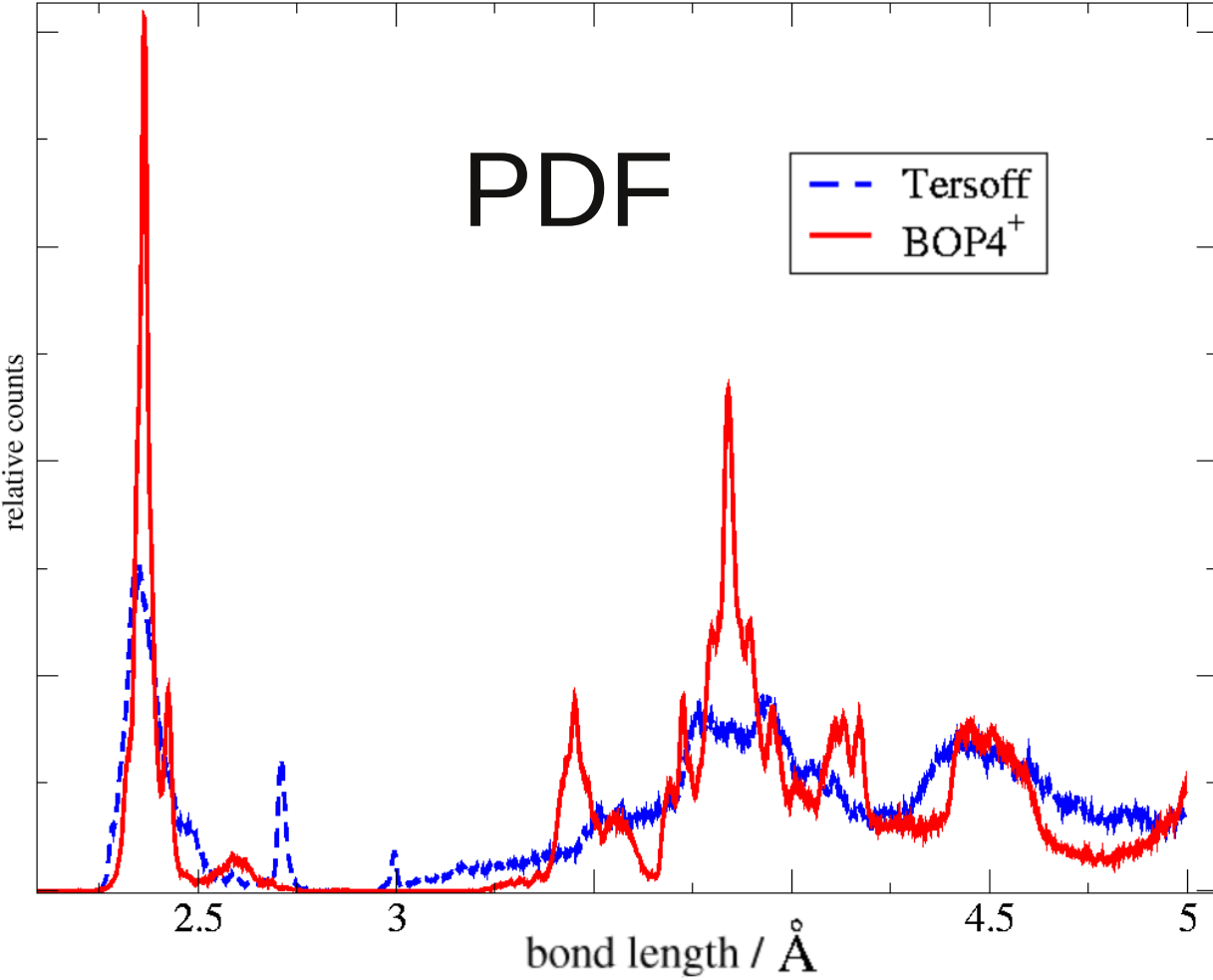
increased stiffness



Si (110) surface
dimerization
0K->600K->0K

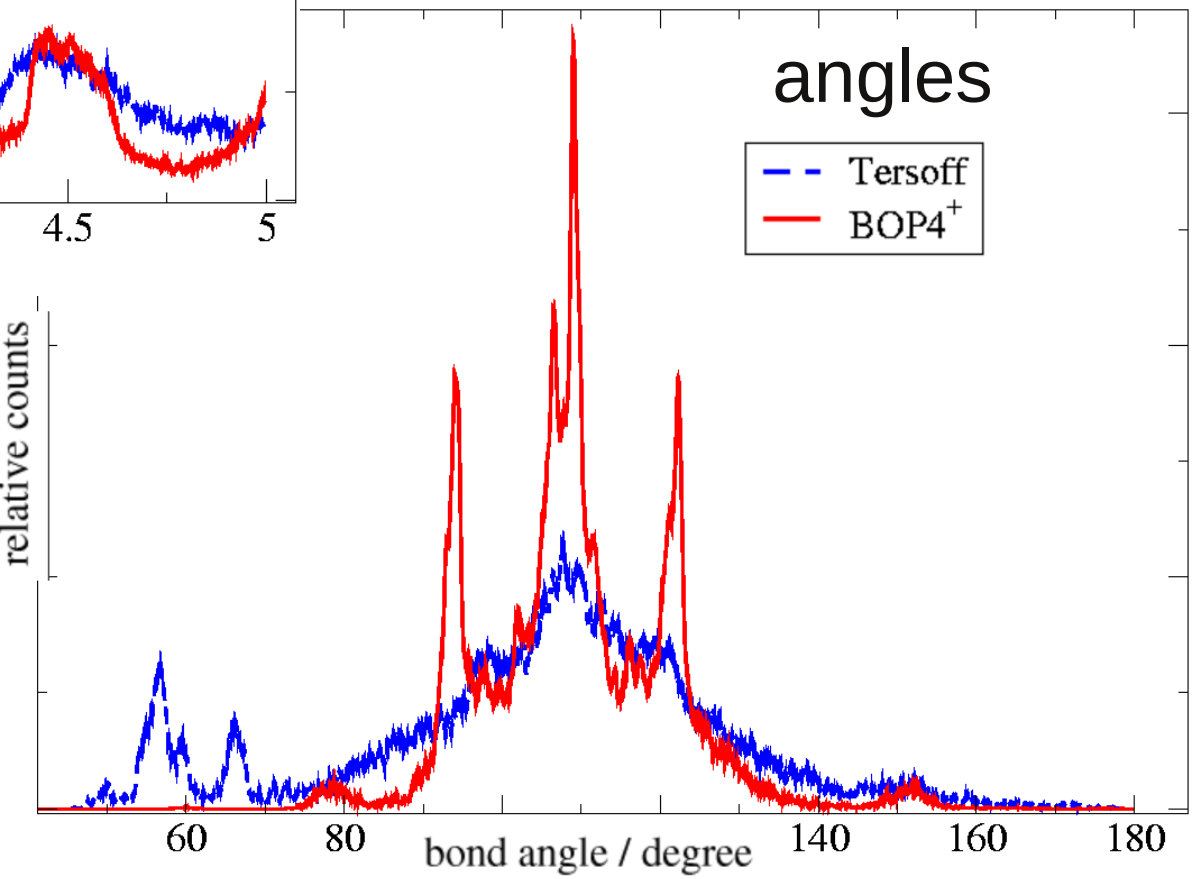


PDF

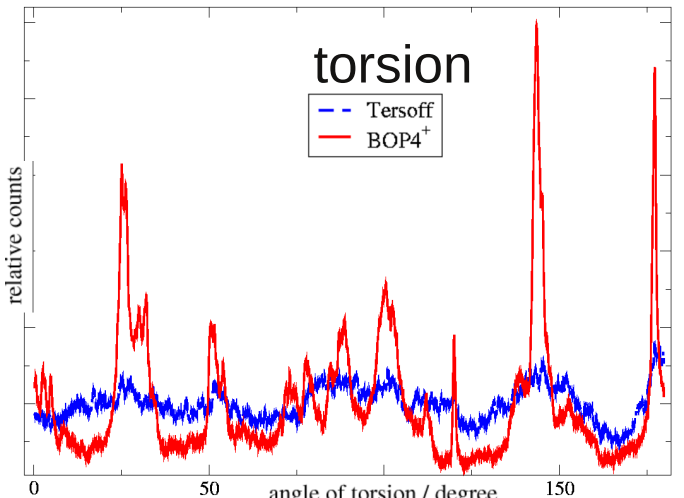


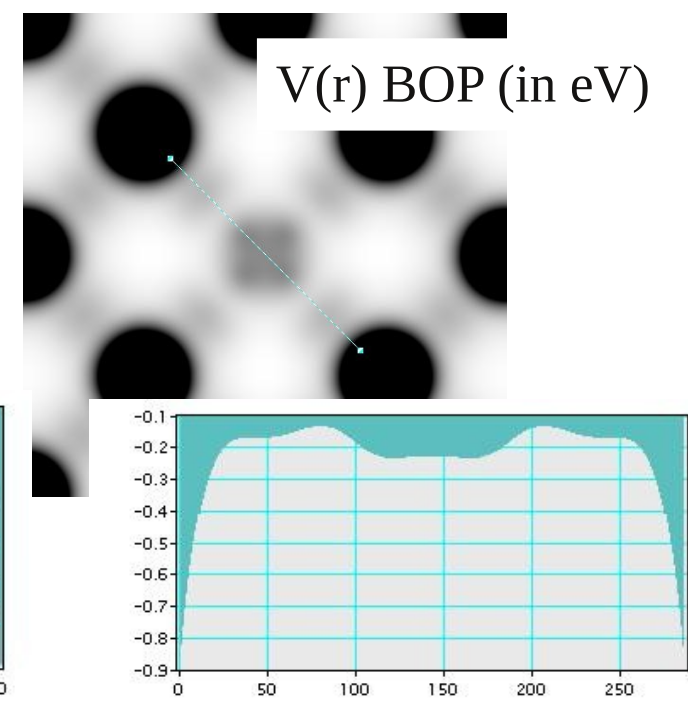
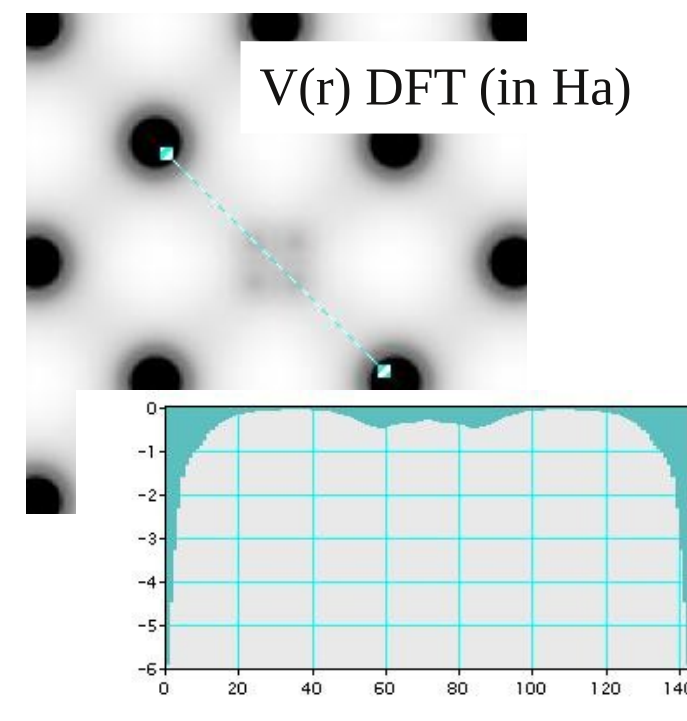
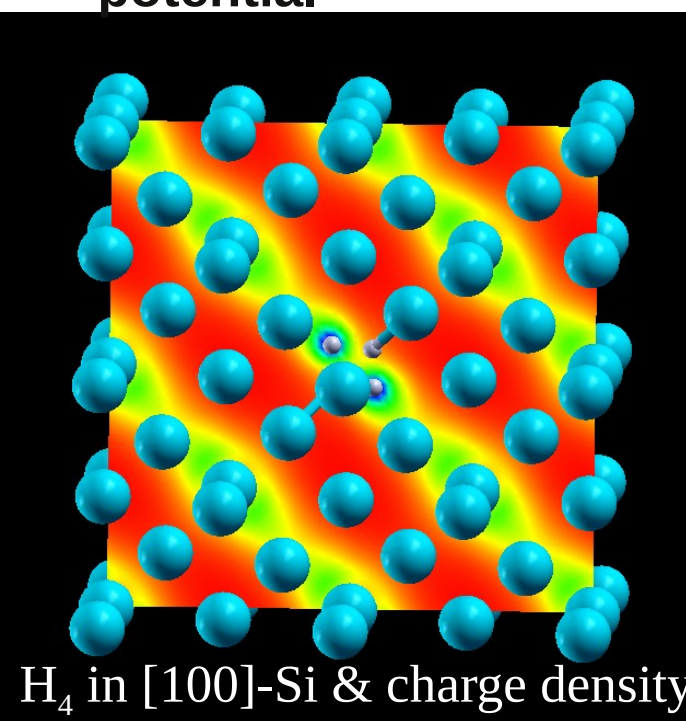
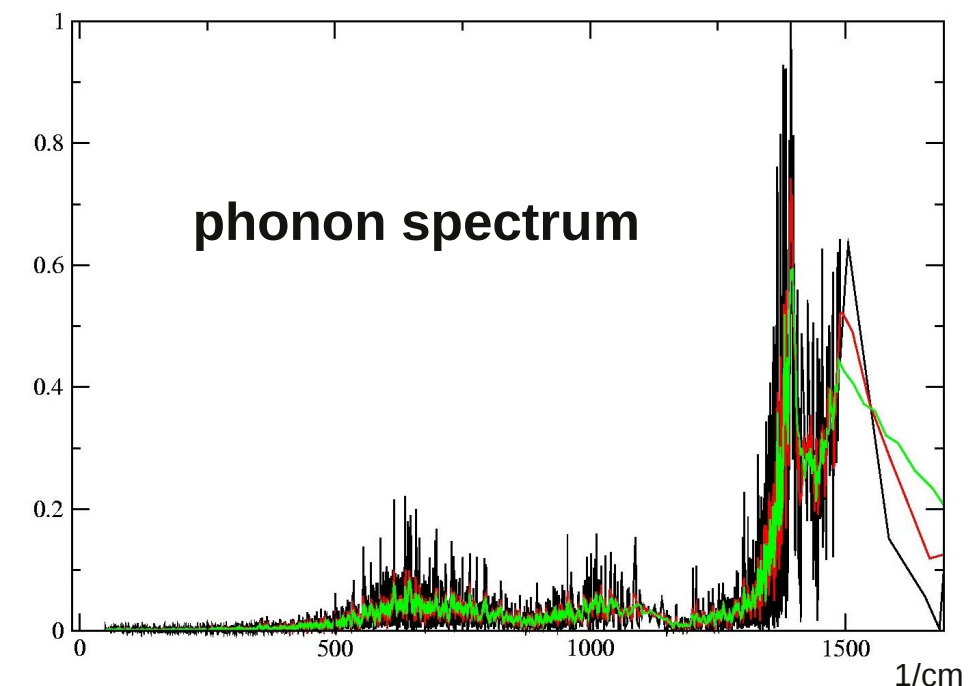
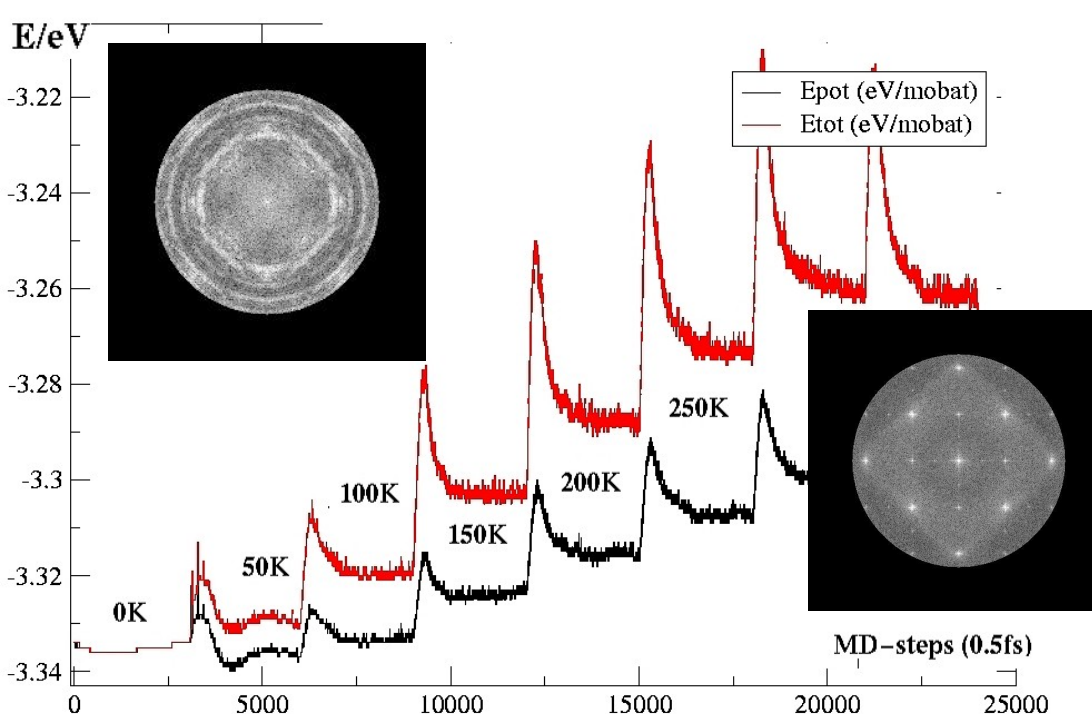
Distribution of pair distances,
angles and torsions at the
1.4° twist bonded Si-001 interface
comparing Tersoff and BOP4+
potentials after annealing at 900K

angles



torsion





Si.95Ge.05

Si.75Ge.25

Si.5Ge.5

Si.25Ge.75

Si.05Ge.95

potential scan

potential average

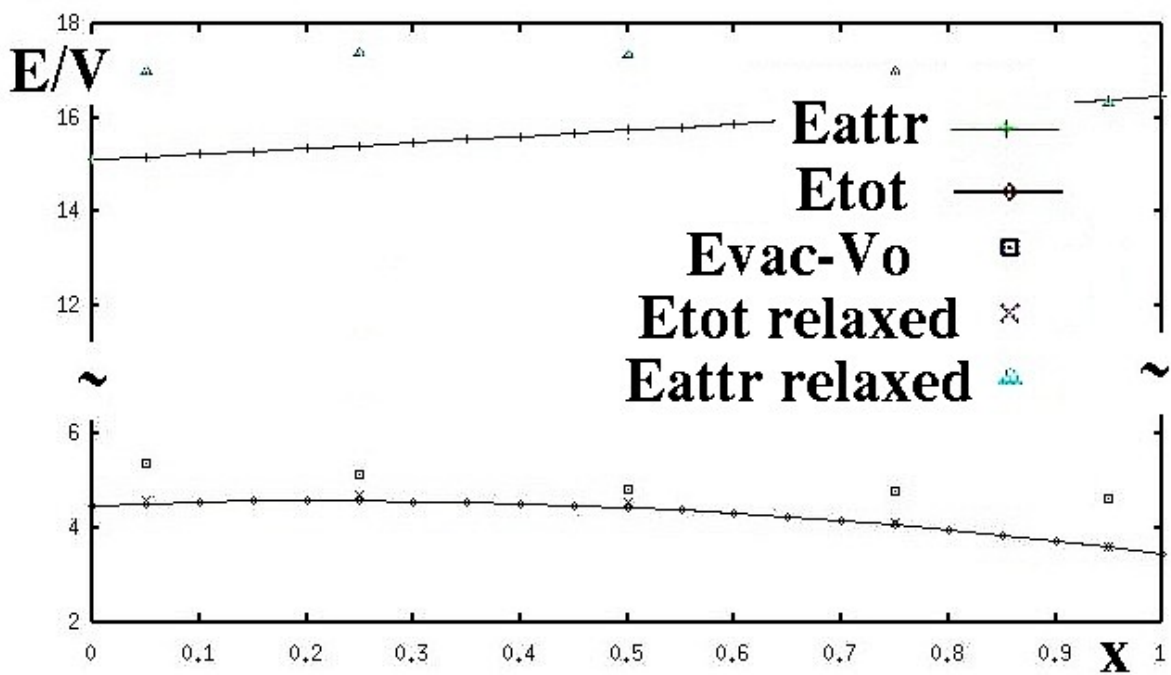
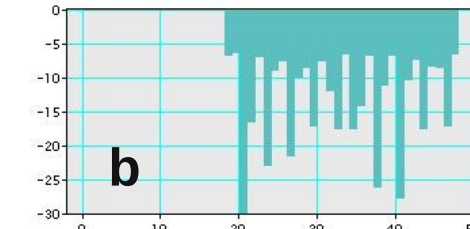
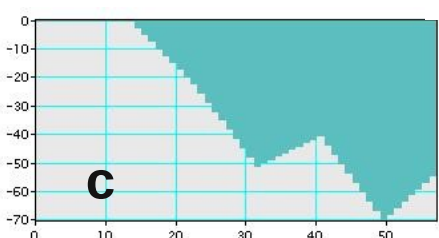
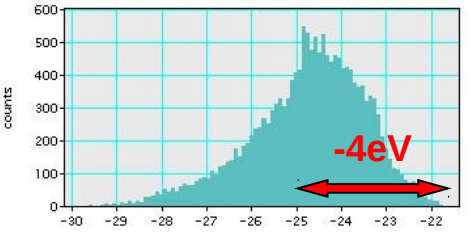
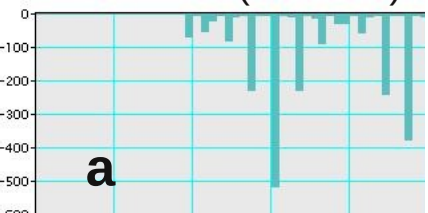
a

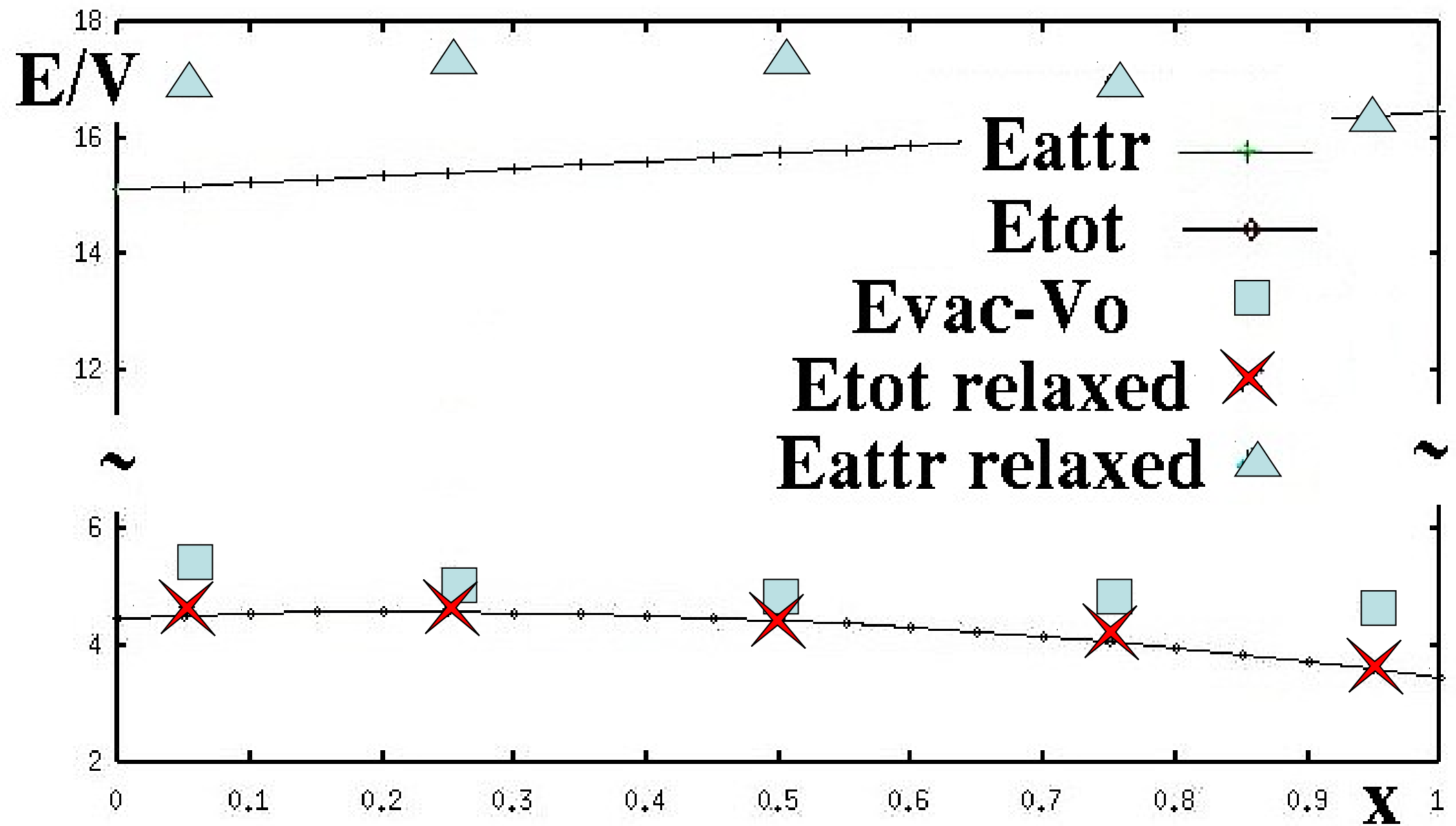
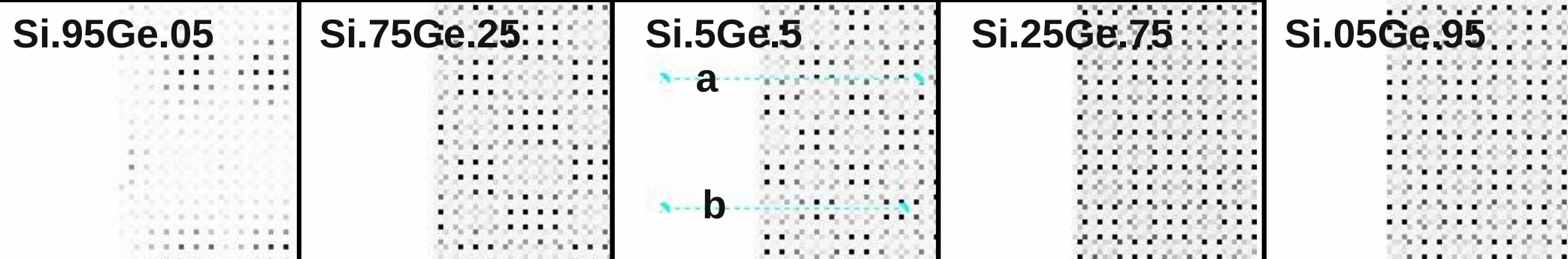
b

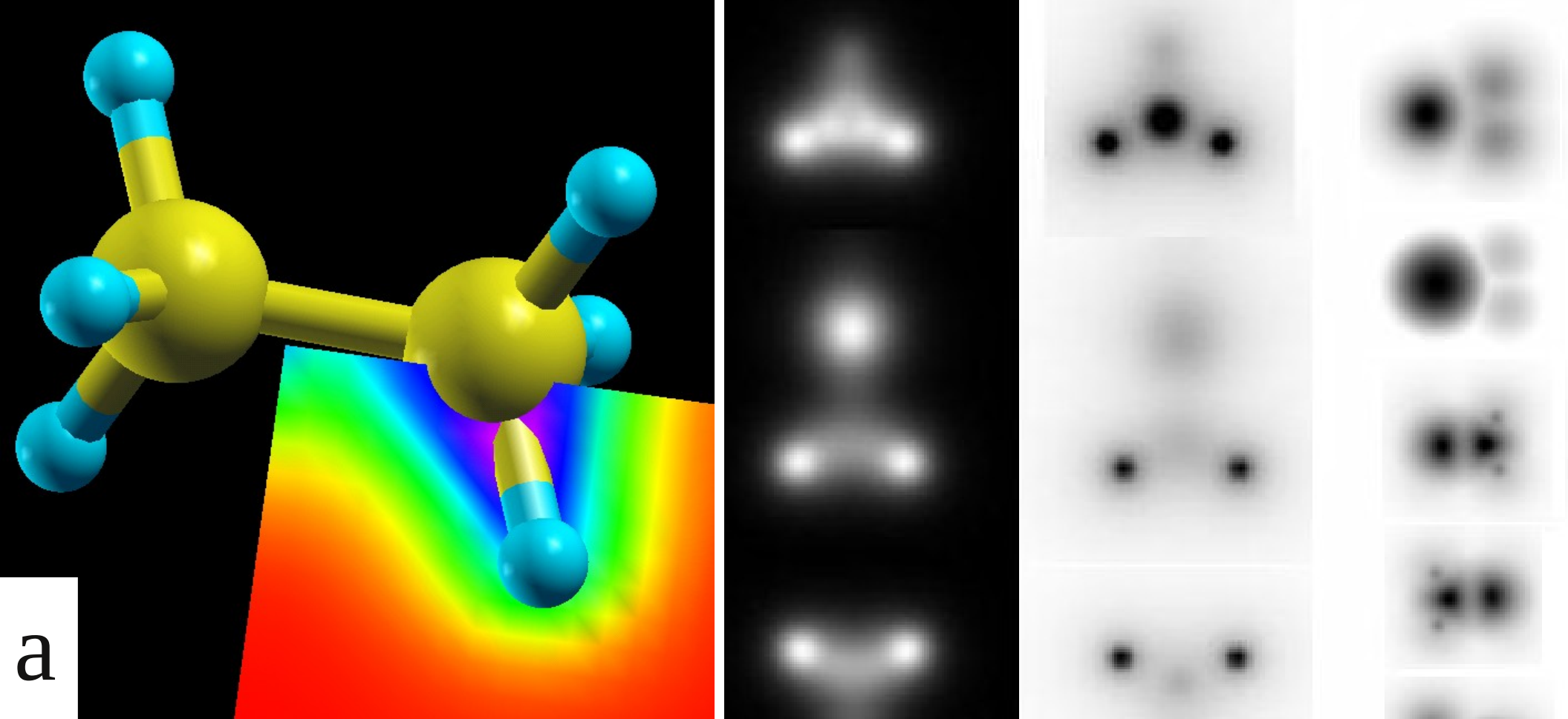
c

d

Si.5Ge.5
background
histogram
(counts/eV)
& linescans (Vo in eV)







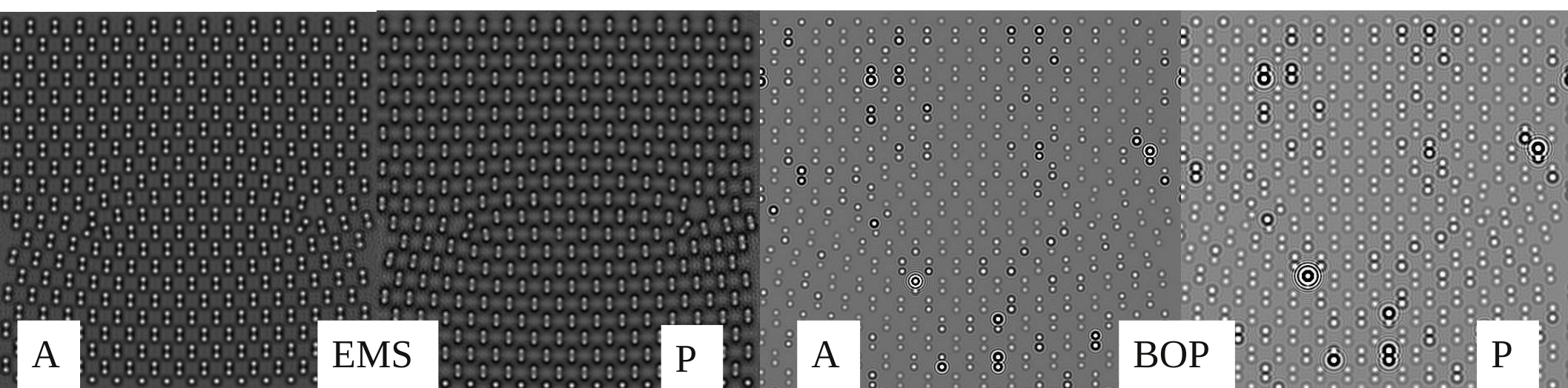
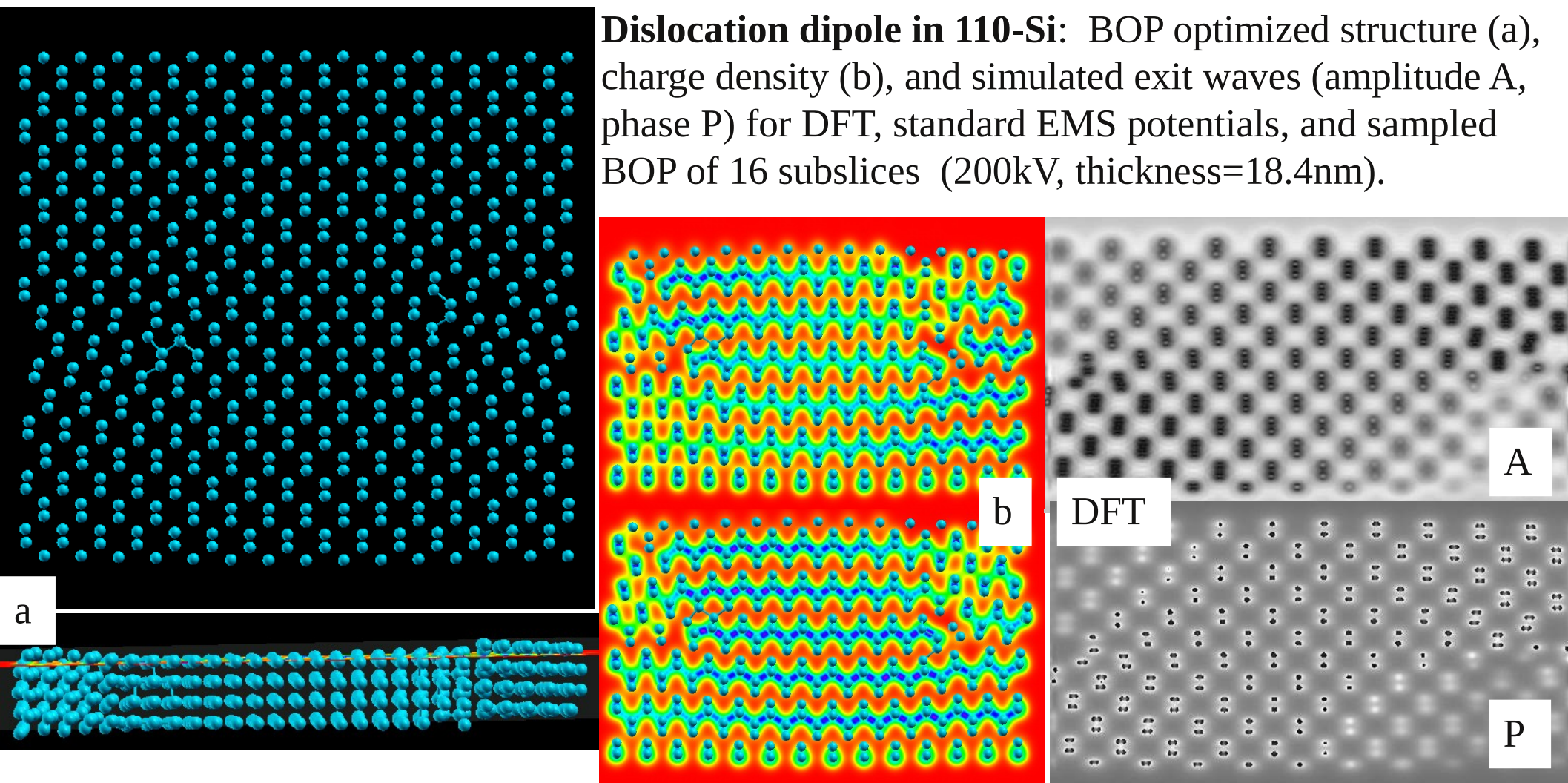
C_2H_6 : DFT-optimized
structure and charge density
(a), selected cuts of density
(b), potential (c), and
sampled BOP (d)

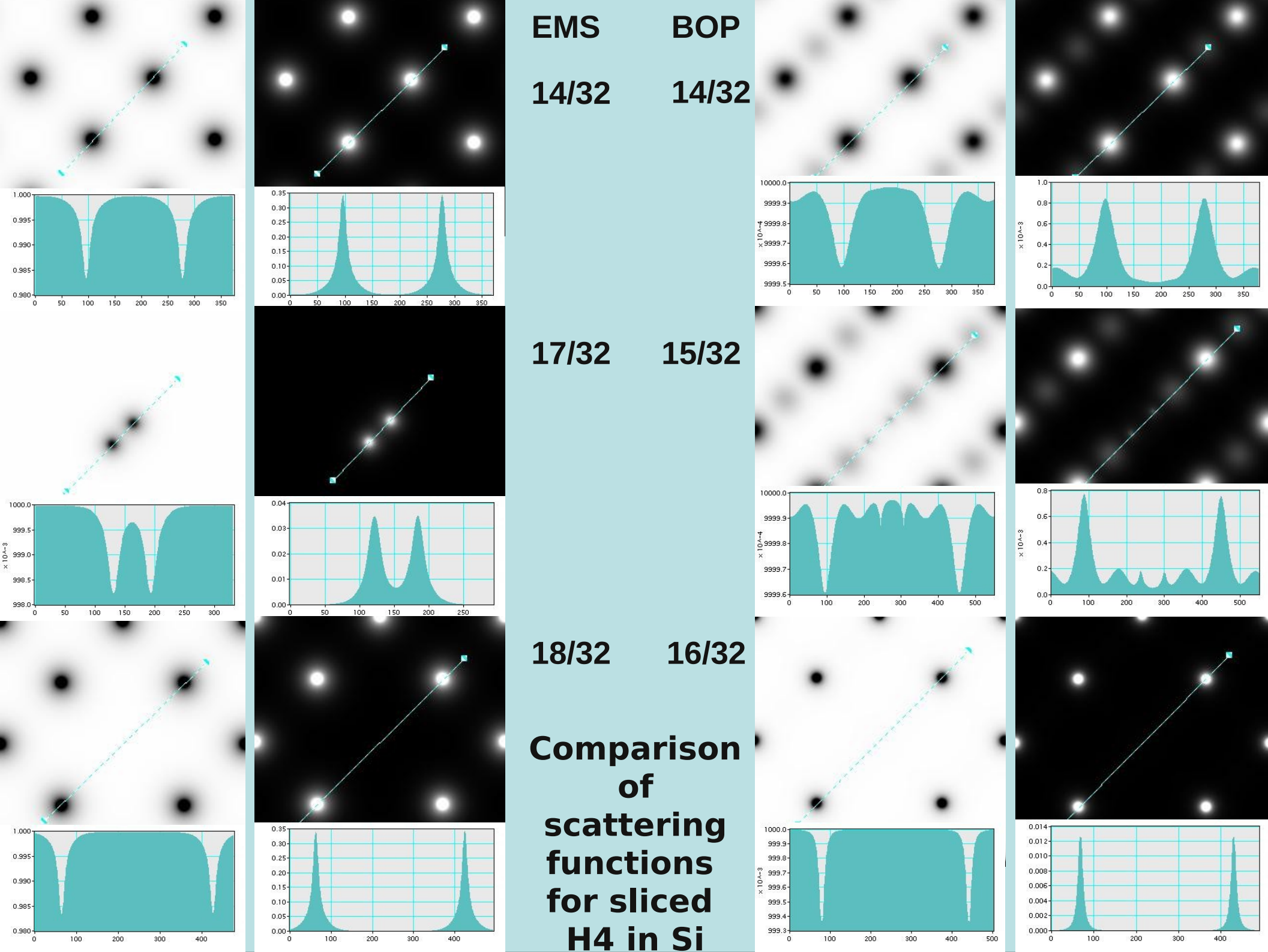
b

c

d

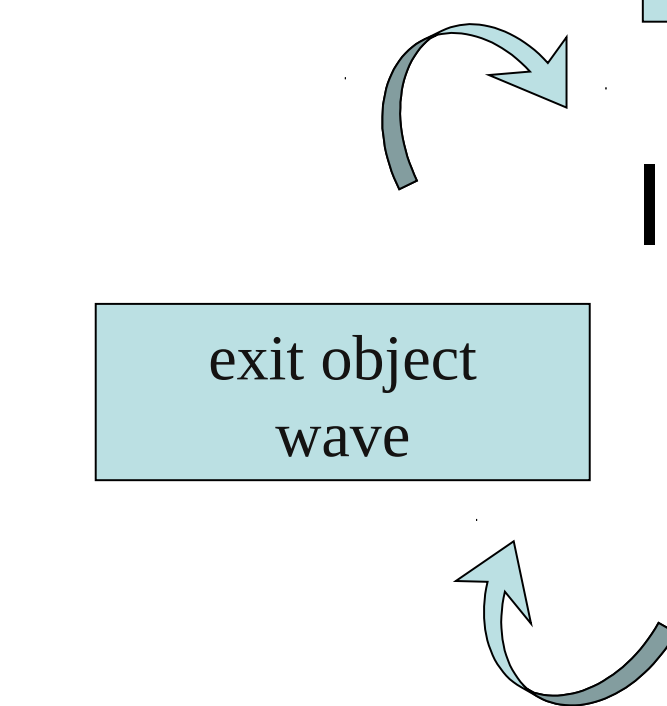
Dislocation dipole in 110-Si: BOP optimized structure (a), charge density (b), and simulated exit waves (amplitude A, phase P) for DFT, standard EMS potentials, and sampled BOP of 16 subslices (200kV, thickness=18.4nm).





multi-slice inversion
(van Dyck, Griblyuk, Lentzen,
Allen, Spargo, Koch)
Pade-inversion (Spence)
non-Convex sets (Spence)
local linearization

deviations from
reference structures:
displacement field (Head)
algebraic discretization

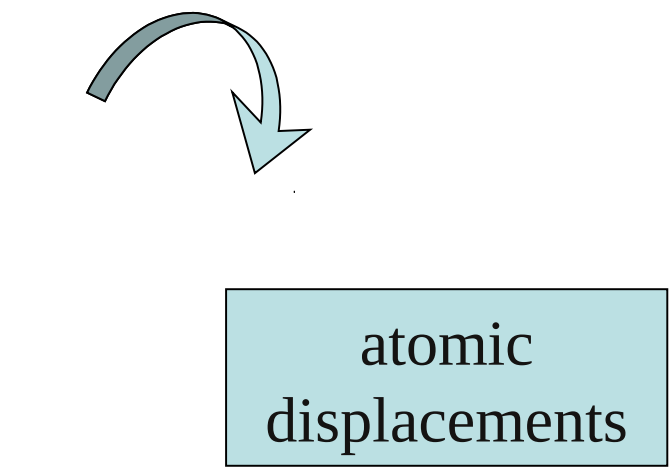


reference beam (holography)
defocus series (Kirkland, van Dyck ...)
Gerchberg-Saxton (Jansson)
tilt-series, voltage variation

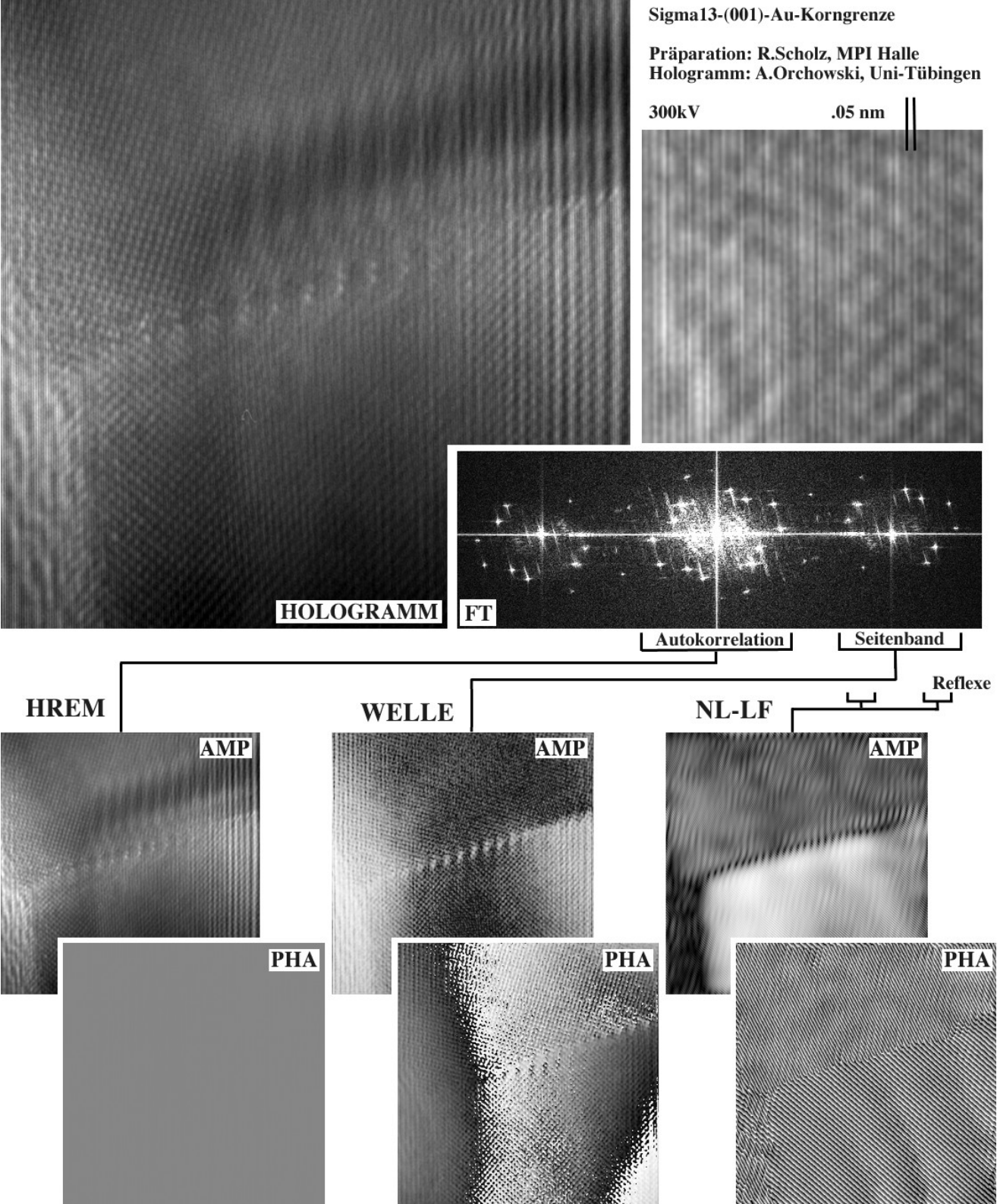
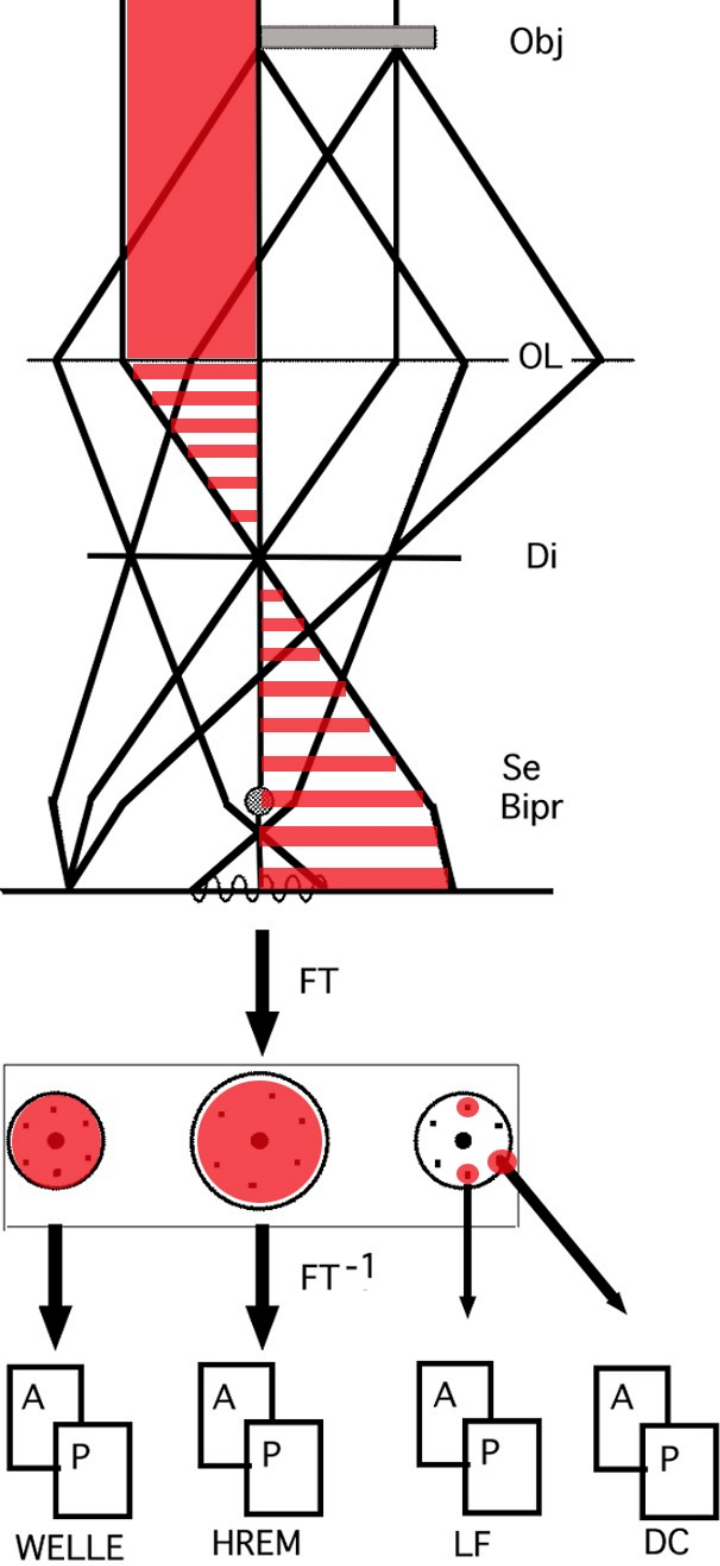


Inversion ?

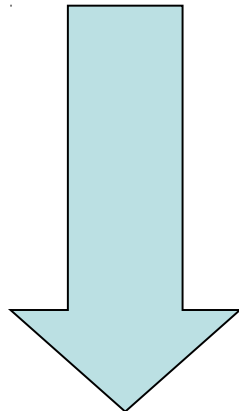
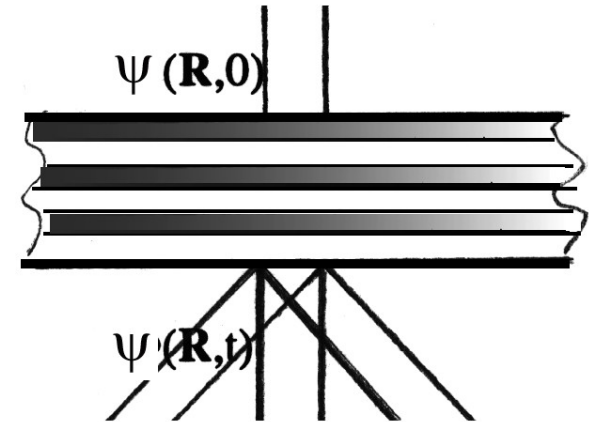
no iteration
same ambiguities
additional instabilities



direct interpretation
by data reduction:
Fourier filtering
QUANTITEM
Fuzzy & Neuro-Net
Strain analysis



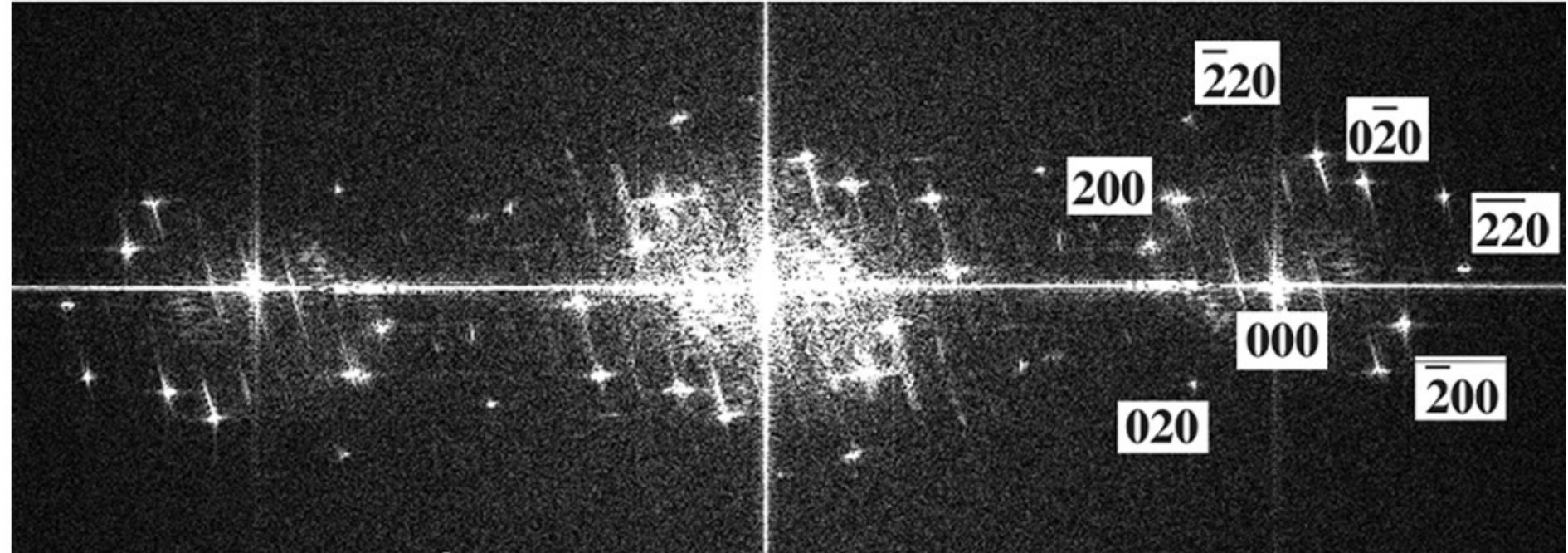
$$\Psi = M(\mathbf{X}) \Psi_0$$



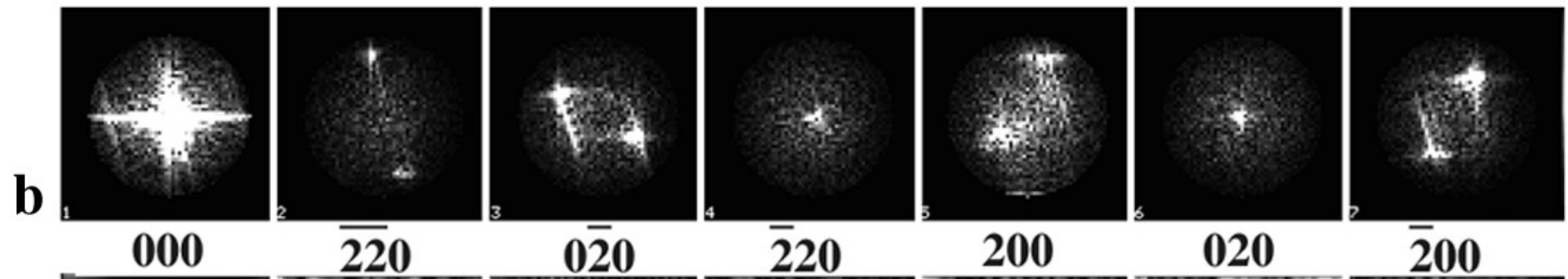
Assumptions:

- object: weakly distorted crystal
- described by unknown parameter set $X = \{t, K, V_g, u\}$
- approximations of t_0, K_0 a priori known

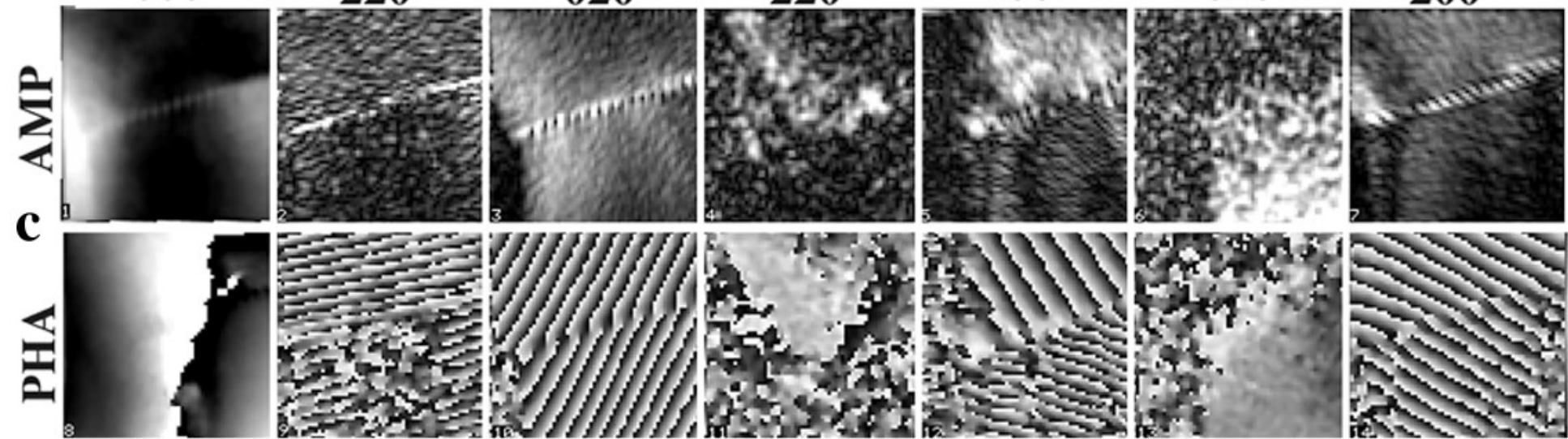
$$\Psi = M(\mathbf{X}_0) \Psi_0 + \vartheta M(\mathbf{X}_0)(\mathbf{X} - \mathbf{X}_0) \Psi_0$$



a

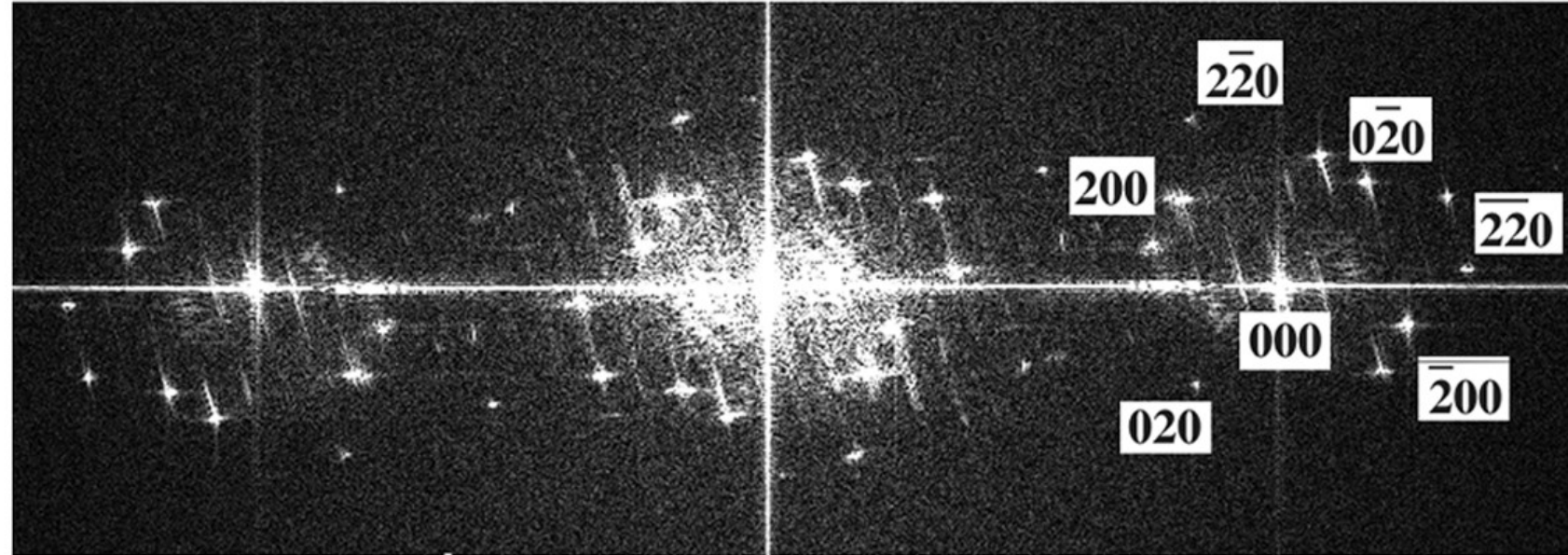


b

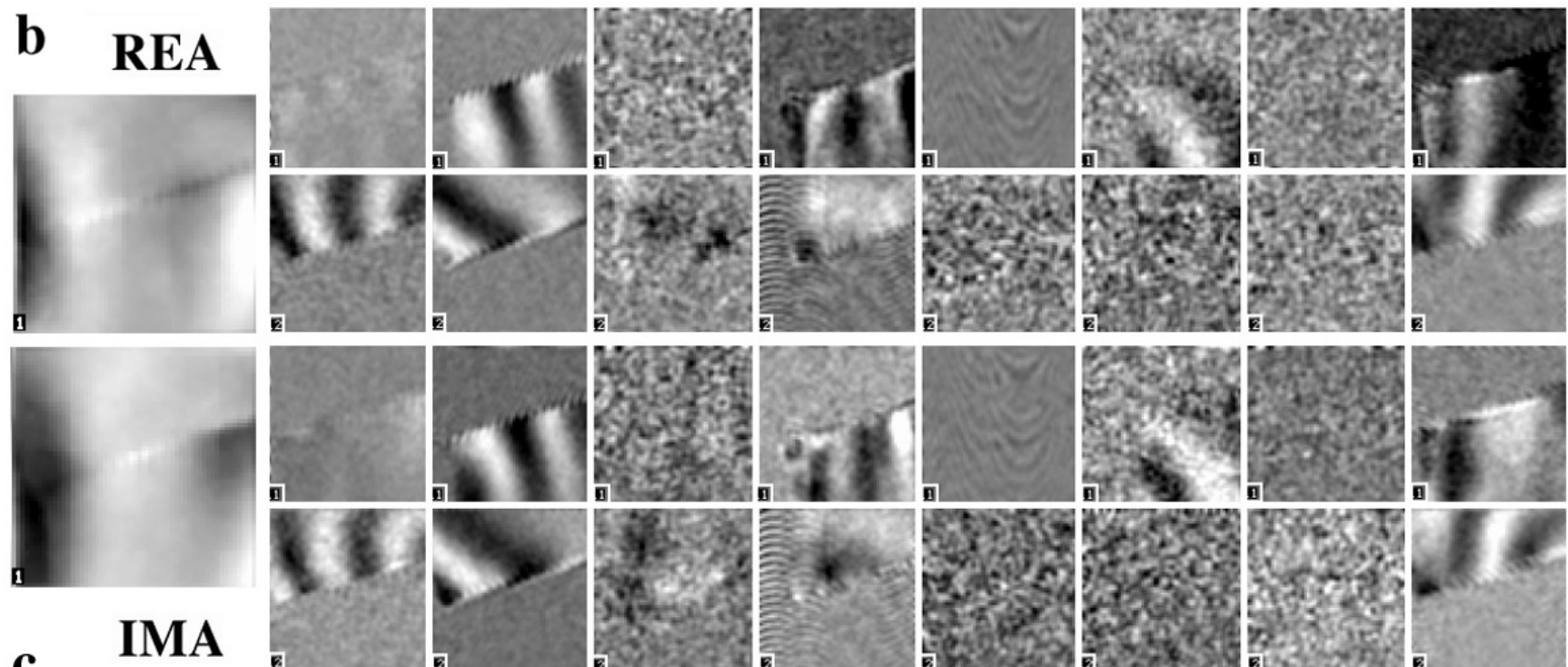


c AMP

PHA



000	$\bar{2}\bar{2}0_1$	$0\bar{2}0_1$	$2\bar{2}0_1$	200_1	220_1	020_1	$\bar{2}20_1$	$\bar{2}00_1$
	$\bar{2}\bar{2}0_2$	$0\bar{2}0_2$	$2\bar{2}0_2$	200_2	220_2	020_2	$\bar{2}20_2$	$\bar{2}00_2$



$$\begin{matrix} A_0 \\ P_0 \end{matrix}$$

$$\begin{matrix} A_{g1} \\ P_{g1} \end{matrix}$$

$$\begin{matrix} A_{g2} \\ P_{g2} \end{matrix}$$

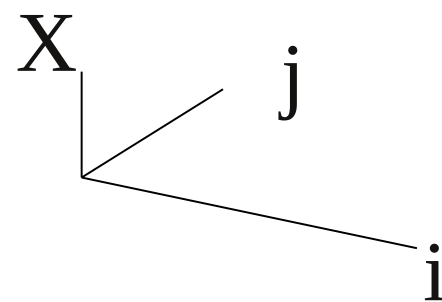
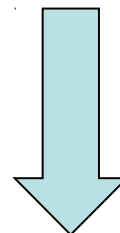
$$\begin{matrix} A_{g3} \\ P_{g3} \end{matrix}$$

...

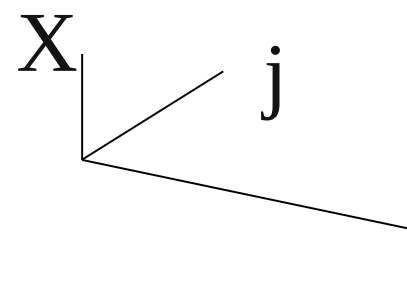


Φ^{exp}

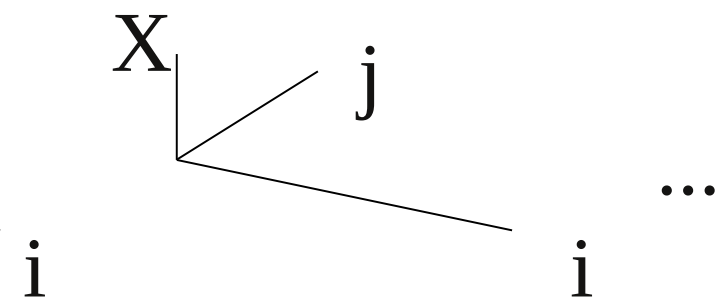
$$X = X_0 + (\nabla M^T \nabla M)^{-1} \nabla M^T \cdot [\Phi^{\text{exp}} - \Phi(X_0)]$$



$$t(i,j)$$

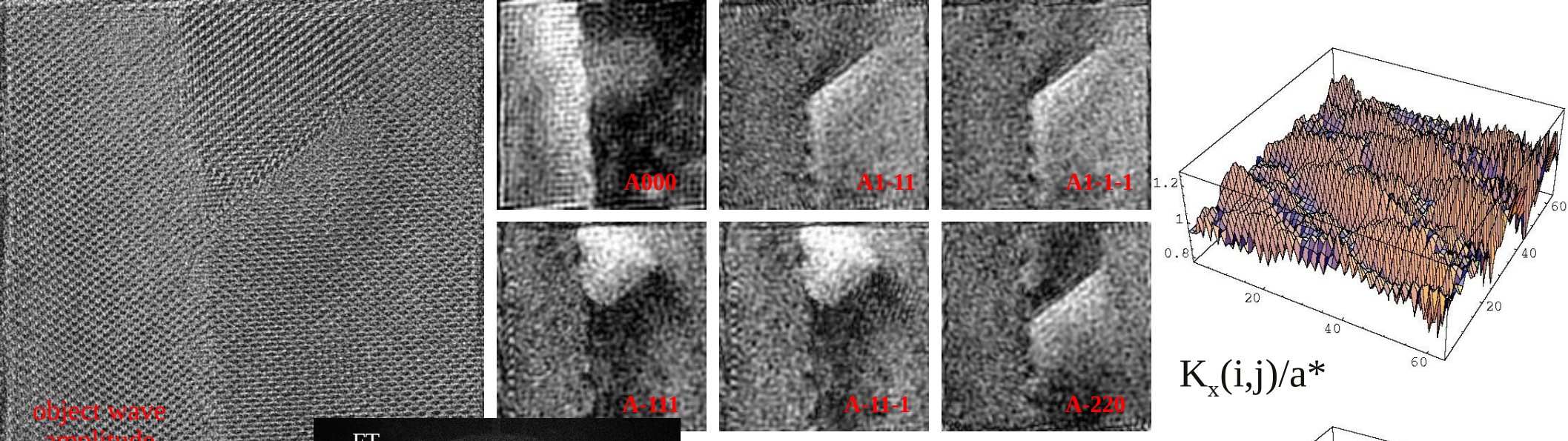


$$K_x(i,j)$$

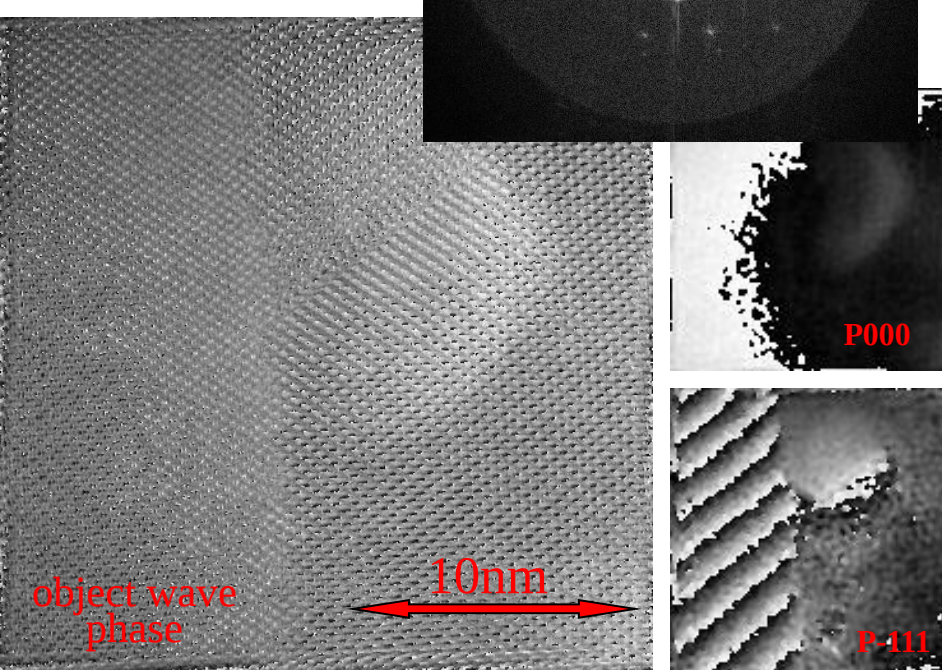


$$K_y(i,j)$$

...



Ge-CdTe, 300kV
 Sample: D. Smith
 Holo: H. Lichte,
 M. Lehmann



set 1: Ge
 set 2: CdTe
 $dV_o/V_o = 0.02\%$
 $dV'_o/V'_o = 0.8\%$

